ACS OMEGA

http://pubs.acs.org/journal/acsodf

Article

Inhibition of Biofilm and Virulence Properties of Pathogenic Bacteria by Silver and Gold Nanoparticles Synthesized from *Lactiplantibacillus* sp. Strain C1

Min-Gyun Kang, Fazlurrahman Khan,* Nazia Tabassum, Kyung-Jin Cho, Du-Min Jo, and Young-Mog Kim*

Cite This: *ACS Omega* 2023, 8, 9873−9888

Read Online

ACCESS | Metrics & More | Article Recommendations | Supporting Information

ABSTRACT: The emergence of antibiotic resistance in microbial pathogens necessitates the development of alternative ways to combat the infections that arise. The current study used nanotechnology as an alternate technique to control virulence characteristics and biofilm development in *Pseudomonas aeruginosa* and *Staphylococcus aureus*. Furthermore, based on the acceptance and biocompatibility of the probiotic bacteria, we chose a lactic acid bacteria (LAB) for synthesizing two types of metallic nanoparticles (NPs) in this study. Using molecular techniques, the LAB strain C1 was isolated from Kimchi food samples and identified as *Lactiplantibacillus* sp. strain C1. The prepared supernatant from strain C1 was used to produce gold nanoparticles (AuNPs) and silver nanoparticles (AgNPs). C1-AuNPs and C1-AgNPs were characterized physiochemically using a variety of instruments. C1-AuNPs and C1-AgNPs had spherical shapes and sizes of 100.54 ± 14.07 nm (AuNPs) and 129.51 ± 12.31 nm (AgNPs), respectively. C1-AuNPs and C1-AgNPs were discovered to have high zeta potentials of −23.29 ± 1.17 and −30.57 ± 0.29 mV, respectively. These nanoparticles have antibacterial properties against several bacterial pathogens. C1-AuNPs and C1-AgNPs significantly inhibited the initial stage biofilm formation and effectively eradicated established mature biofilms of *P. aeruginosa* and *S. aureus*. Furthermore, when *P. aeruginosa* was treated with sub-MIC levels of C1-AuNPs and C1-AgNPs, their different virulence features were significantly reduced. Both NPs greatly inhibited the hemolytic activity of *S. aureus*. The inhibition of *P. aeruginosa* and *S. aureus* biofilms and virulence features by C1-AuNPs and C1-AgNPs can be regarded as viable therapeutic strategies for preventing infections caused by these bacteria.

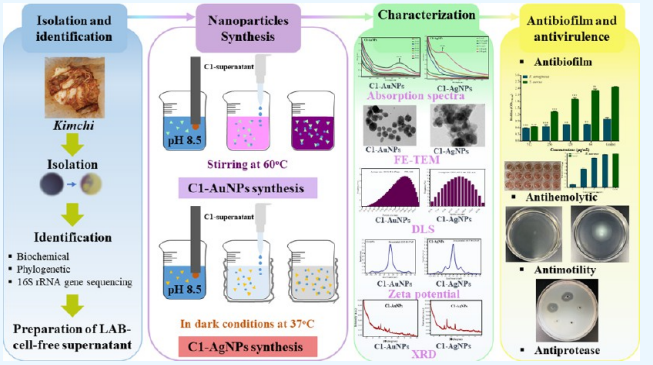

INTRODUCTION

There is an increasing number of reports on the surge of antimicrobial resistance (AMR) traits in various microbial pathogens worldwide.[1] Furthermore, recent studies suggest that AMR from microbial pathogens took a toll on about 4.95 million people.[2] Several research investigations have found that a large variety of bacterial pathogens exhibit diverse resistance mechanisms.[3,4] Biofilm formation is one of the adaptive resistance mechanisms in bacterial pathogens that acts as a primary barrier to drug entrance.[5] Furthermore, these biofilm-forming bacterial pathogens are responsible for the generation of mutants that are selectively more resistant than normal cells.[6,7] The production of several virulence factors further aids pathogenicity and infection by biofilm-forming bacterial pathogens.[8,9] The development of biofilms by pathogenic bacteria on biotic surfaces (e.g., tooth surfaces, skin, trachea, respiratory tract, and urinary tract) and abiotic surfaces (e.g., medical devices and implants) has received considerable attention.[10,11] As a result of the difficulties caused by bacteria that form biofilms, researchers are compelled to investigate alternative infection-fighting methods.[12]

Emerging nanotechnology, notably the use of nanoparticles in managing a wide spectrum of bacterial pathogens, has emerged as a promising strategy.[13] Nanoparticles' features, such as small size, large surface area, biocompatibility, and targeting to specific sites, make them more suited for use in various biochemical functions.[14,15] Most studies used biologically derived raw materials (from algae, fungi, bacteria, and mammals) to synthesize organic or inorganic nanoparticles to treat infectious and noninfectious diseases due to their various benefits over chemically synthesized nanoparticles.[16−19] We

Received: October 21, 2022
Accepted: February 1, 2023
Published: March 7, 2023

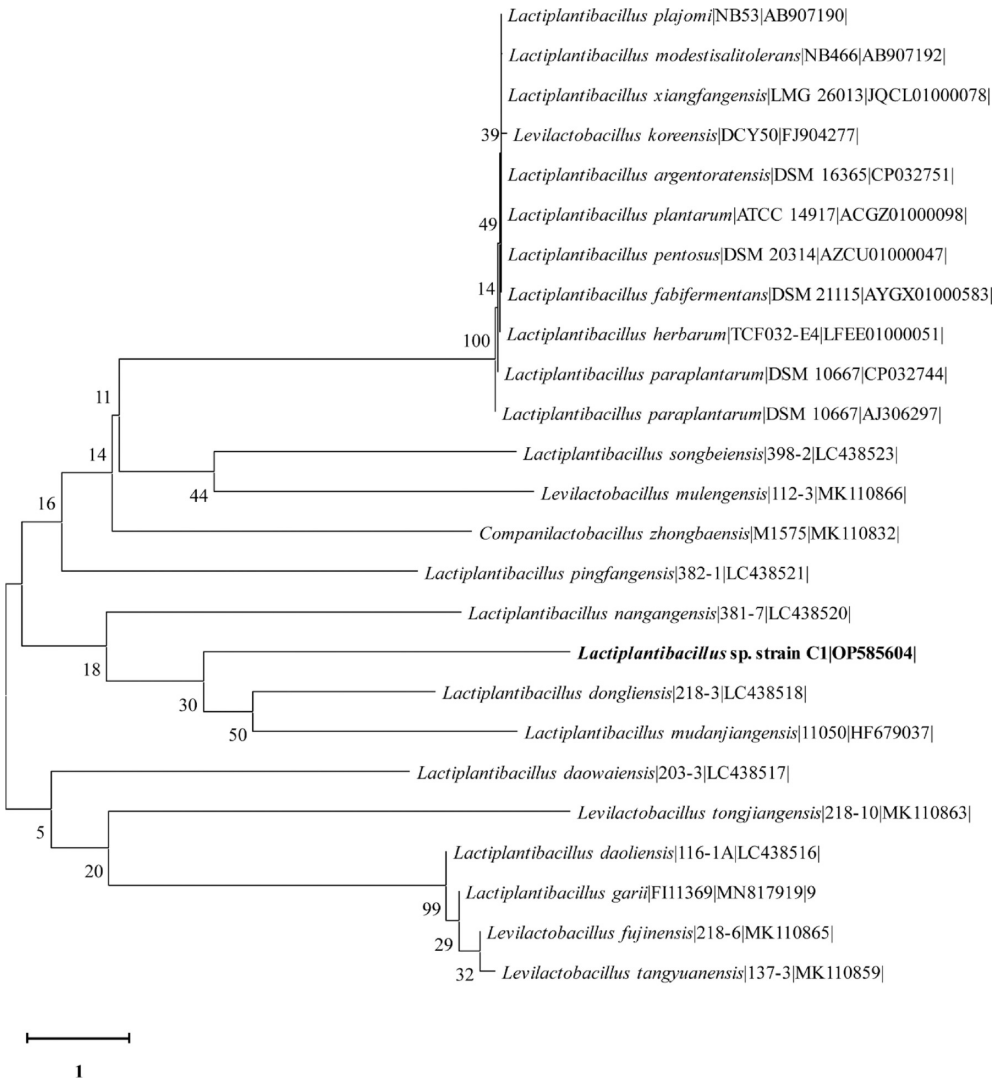

Figure 1. Evolutionary relatedness analysis of the *Lactiplantibacillus* sp. strain C1 with the type strain of LAB based on the 16S rRNA gene sequences.

synthesize two different kinds of metallic nanoparticles, such as silver (AgNPs) and gold (AuNPs), using microbial-derived products as raw materials, which have several advantages. According to a recent study, probiotics, particularly lactic acid bacteria (LAB), have drawn much interest from the food and pharmaceutical industries because of their many advantages for human health and well-being.[20−22] Several studies have shown that LAB provides biological protection against microbial infections.[23,24] As a result, it would be one of the novel approaches to using LAB as an environmentally friendly method of synthesizing biocompatible NPs that can be used to treat a wide variety of microbial infections.[25,26] Thus, in the current study, we sought to isolate and characterize the LAB strains from the Kimchi sample as a biological source for the synthesis of AuNPs and AgNPs. In addition, gas chromatography-mass spectroscopy was used to investigate the identified LAB strain C1 for the production of secondary metabolites to determine their various biological functions.[27]

To investigate biofilm inhibition and virulence properties of synthesized C1-AuNPs and C1-AgNPs, we used one Gram-positive (*Staphylococcus aureus*) and one Gram-negative (*Pseudomonas aeruginosa*) nosocomial biofilm-forming and virulence-producing bacterial pathogen.[8,9] Both *P. aeruginosa* and *S. aureus* are SKAPE bacteria, which are designated as top-priority bacterial pathogens against which novel antibacterial treatments must be identified, according to WHO guidelines.[1,28] The synthesized C1-AuNPs and C1-AgNPs were used to investigate many antibacterial activities against these pathogens, including (1) bactericidal activities, (2) inhibition of early-stage and dispersal of mature biofilms, and (3) reduction of several virulence features.

RESULTS

Lactic Acid Bacteria Isolation and Identification from Kimchi Samples. A total of 15 LAB bacteria were isolated, and their antioxidant properties were evaluated. For the synthesis of AuNPs and AgNPs, strain C1 was chosen because it had the highest antioxidant potential (data not shown). The LAB strain C1 was identified in detail using a molecular technique, which included sequencing the 16S rRNA gene. The 16S rRNA gene sequence obtained was blast searched, and the findings revealed that strain C1 had the most similarities with numerous *Lactiplantibacillus* species. The phylogenetic study also revealed the existence of *Lactiplantibacillus* between its branches (Figure 1). Thus, strain C1 was

https://doi.org/10.1021/acsomega.2c06789
ACS Omega 2023, 8, 9873−9888

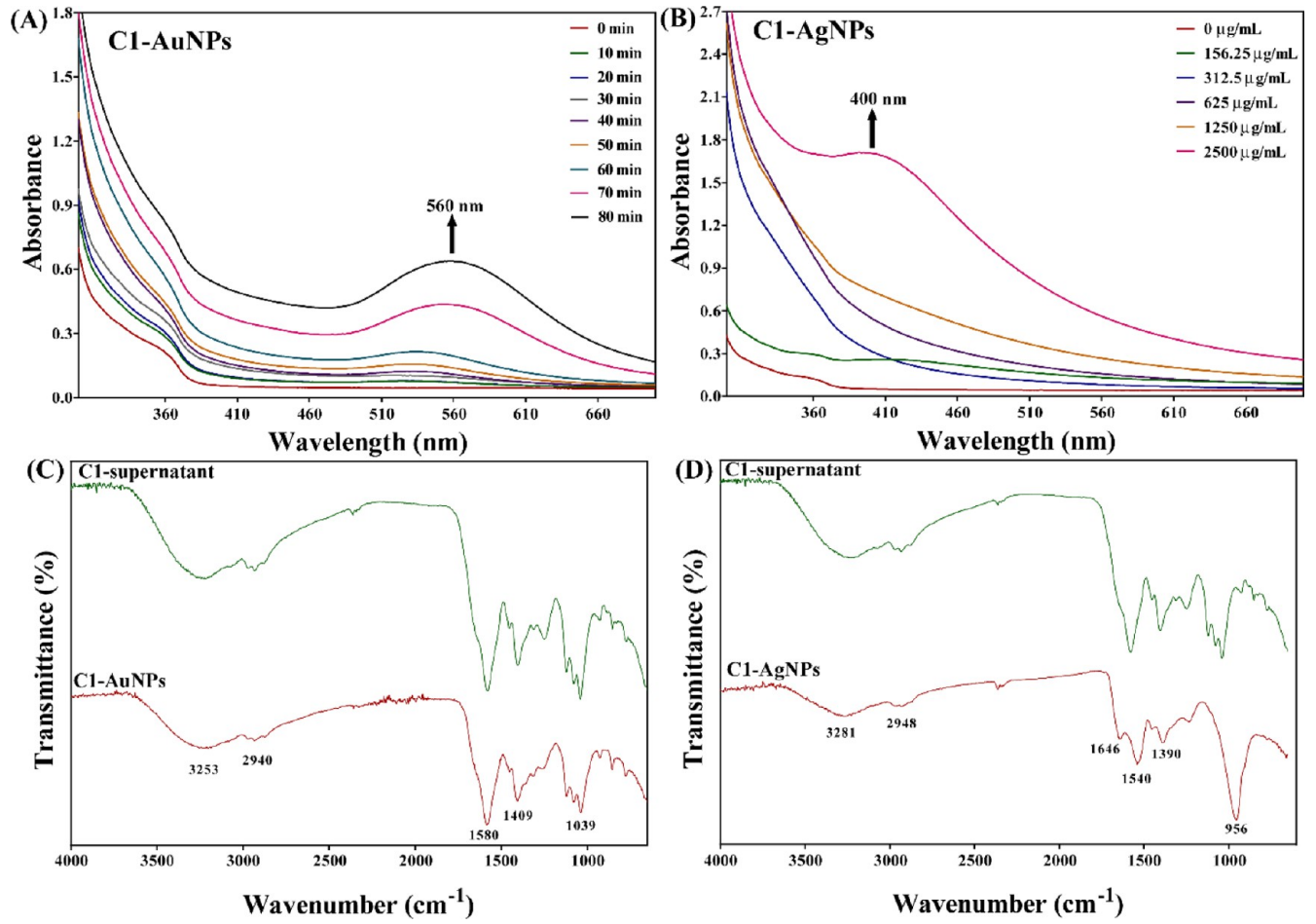

Figure 2. UV−visible absorption spectroscopy and Fourier transform infrared spectroscopy (FTIR) analysis of the NPs. (A) UV−vis absorption spectra of C1-AuNPs, (B) UV−visible absorption spectra of C1-AgNPs, (C) FTIR spectra of C1-AuNPs, and (D) FTIR spectra of C1-AgNPs.

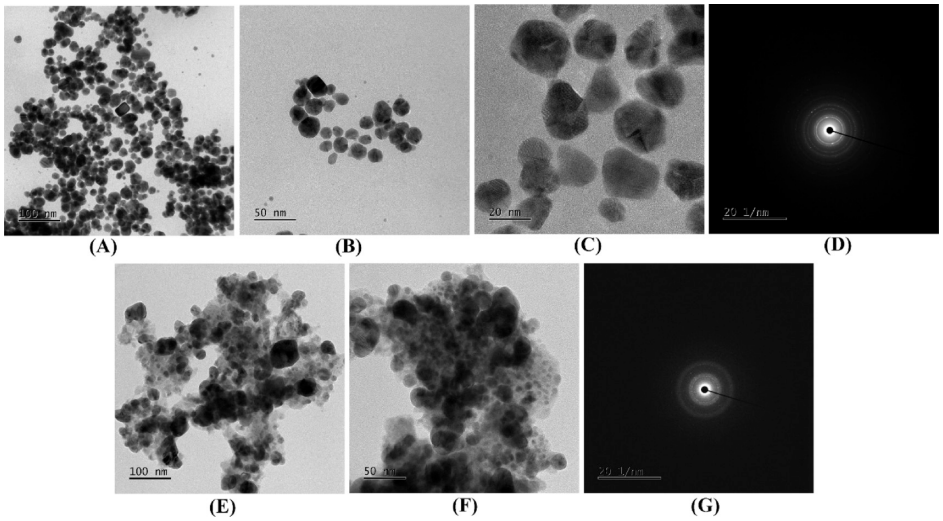

Figure 3. TEM imaging of C1-AuNPs and C1-AgNPs. (A−C) TEM images of C1-AuNPs at 100, 50, and 20 nm resolution, (D) SAED of C1-AuNPs, (E,F) TEM images of C1-AgNPs at 100 and 50 nm resolution, and (G) SAED of C1-AgNPs.

identified as *Lactiplantibacillus* sp. strain C1 based on 16S rRNA gene sequencing and phylogenetic analysis. The strain C1 16S rRNA gene sequence has been submitted to NCBI GenBank as accession number OP585604.

Green Synthesis of C1-AuNPs and C1-AgNPs. The initial confirmation for the formation of C1-AuNPs was based on the color transition from yellow to red wine, whereas there was white precipitation in the case of C1−AgNP formation. Furthermore, *in situ* spectral scanning was performed, and the results revealed that there was a rising absorption peak at 560 nm in the case of the C1-AuNPs (Figure 2A), whereas a

https://doi.org/10.1021/acsomega.2c06789
ACS Omega 2023, 8, 9873−9888

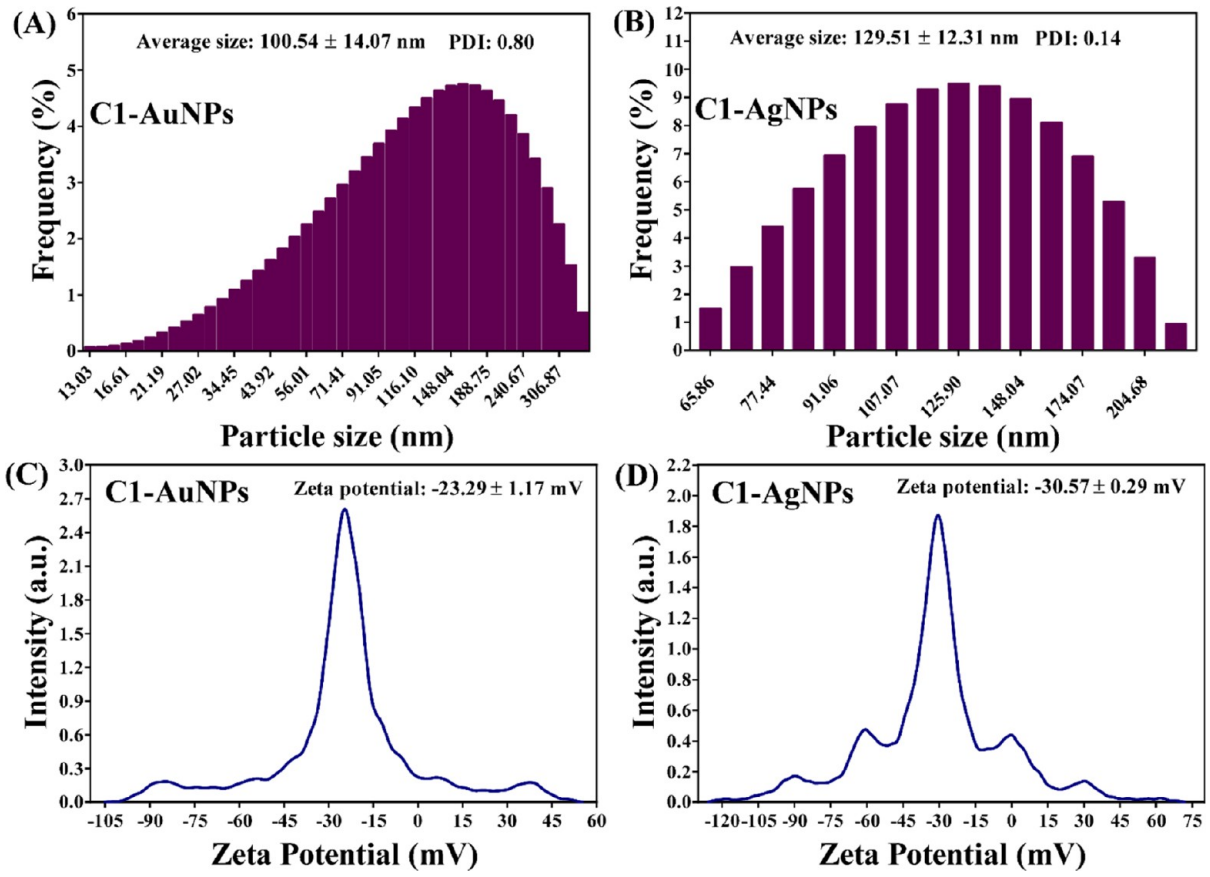

Figure 4. (A) Particle size distribution of C1-AuNPs, (B) particle size distribution of C1-AgNPs, (C) zeta potential of C1-AuNPs, and (D) zeta potential of C1-AgNPs.

400 nm absorption peak in the case of the C1-AgNPs (Figure 2B) is indicating the production of these NPs.

These absorption peaks at the specific wavelength were continually growing as the reaction time increased. To determine the ionic interaction, FTIR analysis was also performed. The FTIR data revealed that the C1 supernatant has certain vibration band characteristics (Figure 2C,D). Some comparable FTIR spectra in the cases of C1-AuNPs and C1-AgNPs have also been found, indicating the interaction of the supernatant component with the produced NPs. The distinctive vibration bands in the FTIR spectra of C1-AuNPs were found to be at 3253, 2940, 1580, 1409, and 1039 cm^{-1} (Figure 2C). Similar spectra were discovered in the FTIR analysis of AuNPs synthesized from various other natural materials.[29,30] The broad band at 3253 cm^{-1} represents O−H stretching, the band at 2940 cm^{-1} represents the presence of the C−H stretch of the alkane group, the band at 1580 cm^{-1} for the C−N, the band at 1409 cm^{-1} for the C−H, and the band at 1039 cm^{-1} shows the C−N stretch of aliphatic amines.[30] Similar types of FTIR spectra in the case of C1-AgNPs have also been observed, which are recognized AgNP characteristics. The particular bands were found to be present at 3281, 2948, 1646, 1540, 1390, and 956 cm^{-1}, respectively (Figure 2D). These observed bands have also been found in the FTIR spectra of AgNPs produced from various natural sources.[31] The broad band at 3253 cm^{-1} represents O−H stretching, the band at 2940 cm^{-1} represents the presence of the C−H stretch of the alkane group, the band at 1580 cm^{-1} represents the presence of the C−N, the band at 1409 cm^{-1} represents the existence of the C−H bond. The band at 1039 cm^{-1} represents the presence of the C−N stretch of aliphatic amines.

Field emission-transmission electron microscopy (FE-TEM) helped examine the morphology of the produced C1-AuNPs and C1-AgNPs, as shown in Figure 3. The morphology of C1-AuNPs was found to be spherical (Figure 3A−C). Similarly, C1-AgNPs were found to have a spherical shape (Figure 3E,F). The size of C1-AuNPs and C1-AgNPs was measured using a particle analyzer (Figure 4A,B). C1-AuNPs had an average size of 100.54 ± 14.07 nm and a polydispersity index (PDI) of 0.80 (Figure 4A). C1-AgNPs were observed to have an average size of 129.51 ± 12.31 and a PDI value of 0.14 (Figure 4B). The zeta potential was used to determine the presence of charge on C1-AuNPs and C1-AgNPs. The zeta potential of C1-AuNPs was determined to be −23.29 ± 1.17 mV (Figure 4C), while the zeta potential of C1-AgNPs was found to be −30.57 ± 0.29 mV (Figure 4D).

The elemental composition of the produced NPs was determined using energy dispersive X-ray spectroscopy (EDS). The scanning electron microscopy (SEM) picture acquired in the EDS also demonstrates the spherical shape of C1-AuNPs (Figure 5A), and Au peaks in the spectra indicate the presence of Au in C1-AuNPs (Figure 5B). The mapping of Au by EDS also shows the existence of Au in C1-AuNPs (Figure 5C). The SEM image of C1-AgNPs obtained in the EDS further verifies their spherical shape (Figure 5E). The presence and composition of Ag in C1-AgNPs were verified by EDS spectra (Figure 5D). The presence of Ag in the C1-AgNPs was further verified by the mapping of Ag using EDS (Figure 5F).

https://doi.org/10.1021/acsomega.2c06789
ACS Omega 2023, 8, 9873−9888

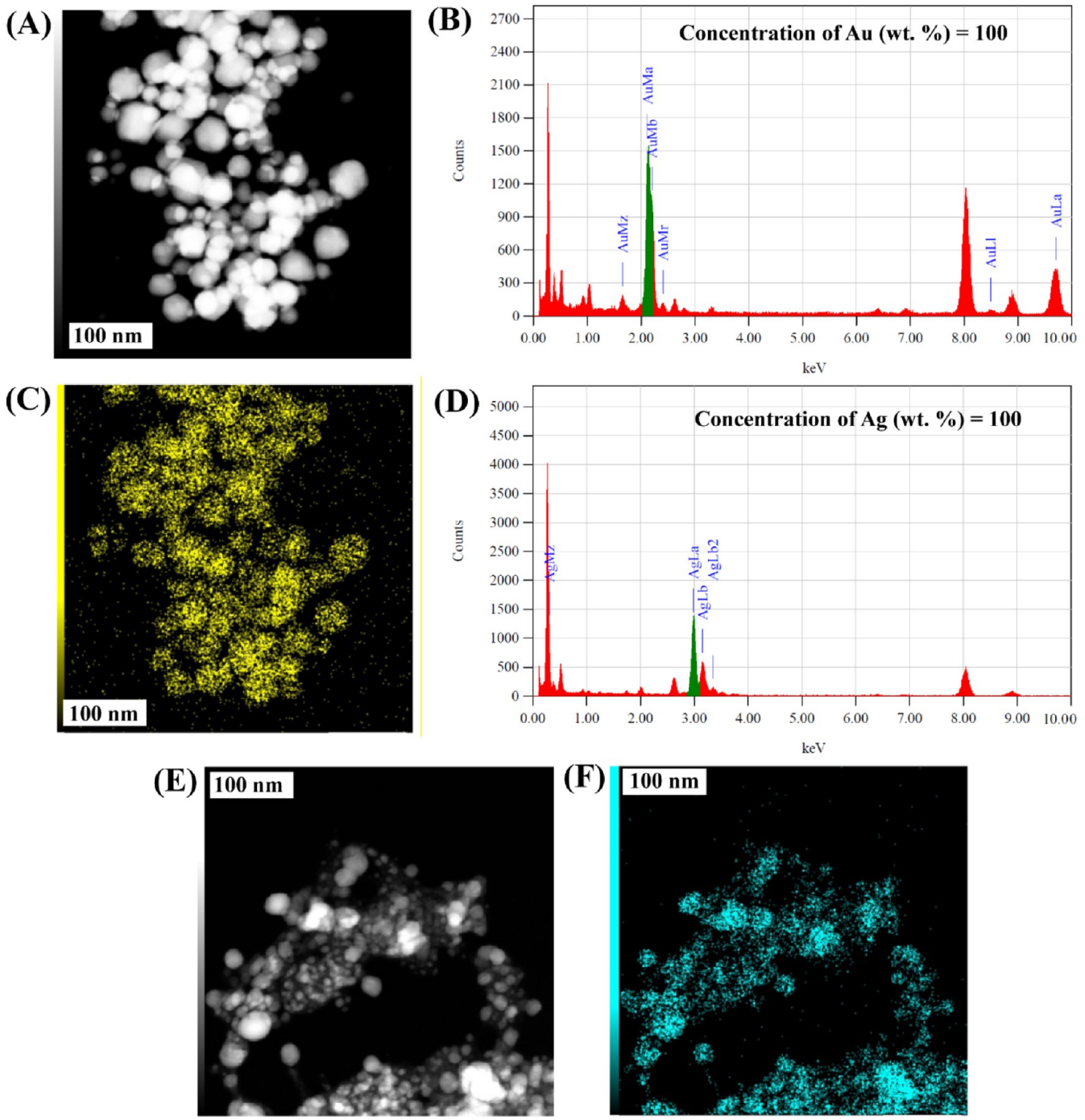

Figure 5. (A) SEM image of C1-AuNPs, (B) EDS spectrum of C1-AuNPs, (C) Au elemental map from C1-AuNPs, (D) EDS spectrum of C1-AgNPs, (E) SEM image of C1-AgNPs, and (F) Ag elemental map from C1-AgNPs.

The crystallinity of the produced NPs was also confirmed by X-ray diffractometry (XRD) (Figure 6). Only a few wide peaks have been identified in the XRD spectra of C1 supernatant between 16 and 28° (Figure 6A). The XRD spectra of the C1-AuNPs were found to be present distinct diffraction peaks at 2θ values of 38.2, 45.6, 50.6, 56.3, 64.4, 75.1, 77.6, and 83.8° (Figure 6B). Similarly, the C1-AgNPs XRD spectra indicate the existence of distinctive diffraction peaks at 2θ values of 38.1, 46.1, 64.2, and 76.9° (Figure 6C). These distinct diffraction peaks in C1-AuNPs and C1-AgNPs have previously been shown to be common in AuNPs and AgNPs synthesized from various materials.

Microbial Efficacy of the Supernatant and the Metallic Nanoparticles. C1 supernatant and nanoparticles such as C1-AuNPs and C1-AgNPs were tested for antibacterial properties towards various bacterial species (detailed in Table 1). The MIC values were determined when cell growth inhibition was greater than 90%, which was also confirmed by a visual assessment of the cell turbidity in each well. C1 supernatant MIC values against all tested bacterial pathogens were determined to be 4096 μg/mL. On the other hand, C1-AuNPs and C1-AgNPs showed varied MIC values for each bacterial pathogen (Table 1). C1-AuNPs had MIC values of 2048 μg/mL against *Listeria monocytogenes* and 1024 μg/mL

https://doi.org/10.1021/acsomega.2c06789
ACS Omega 2023, 8, 9873−9888

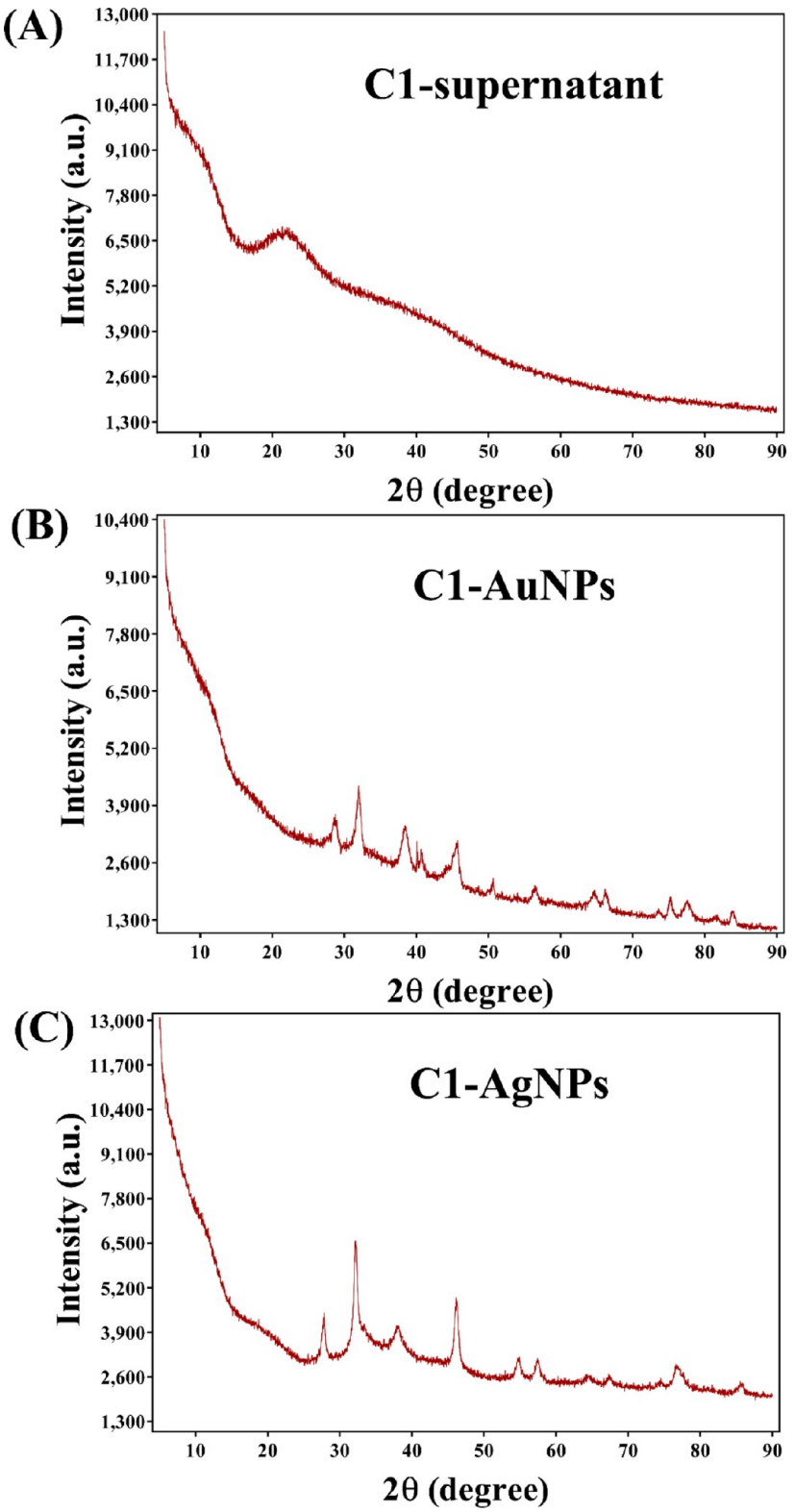

Figure 6. (A) XRD spectra of the C1 supernatant, (B) XRD spectra of C1-AuNPs, and (C) XRD spectra of C1-AgNPs.

against *S. aureus* and *P. aeruginosa*. The MIC values for *Streptococcus mutans*, *Escherichia coli*, and *Klebsiella pneumoniae* were determined to be 256 μg/mL. In comparison to C1-AuNPs, the MIC values of C1-AgNPs against all pathogens were found to be lower. C1-AgNPs had a MIC of 256 μg/mL against *L. monocytogenes* but only 128 μg/mL against *S. aureus*, *E. coli*, and *K. pneumoniae* (Table 1). Based on the findings, it is inferred that the synthesized NPs exhibit lower MIC values against microbial pathogens than the C1 supernatant. The minimum bactericidal concentration (MBC) of both NPs, including the antibiotic control tetracycline, and C1 supernatant, was one-fold higher than MIC values (Table 1). Furthermore, each NP, including C1 supernatant and tetracycline, was found to have a bactericidal effect against

https://doi.org/10.1021/acsomega.2c06789
ACS Omega 2023, 8, 9873−9888

Table 1. MIC, MBC, and MBC/MIC Values of C1 Supernatant, C1-AuNPs, C1-AgNPs, and Tetracycline (Positive Control) against Different Pathogenic Bacteria[a]

	antibacterial activities											
	C1 supernatant			C1-AuNPs			C1-AgNPs			tetracycline		
pathogens	MIC (μg/mL)	MBC (μg/mL)	MBC/MIC ratio	MIC (μg/mL)	MBC (μg/mL)	MBC/MIC ratio	MIC (μg/mL)	MBC (μg/mL)	MBC/MIC ratio	MIC (μg/mL)	MBC (μg/mL)	MBC/MIC ratio
S. mutans	4096	8196	2	256	512	2	32	64	2	0.5	1	2
S. aureus	4096	8196	2	1024	2048	2	128	256	2	0.25	0.5	2
P. aeruginosa	4096	8196	2	1024	2048	2	32	64	2	16	16	1
E. coli	4096	8196	2	256	512	2	128	256	2	1	2	2
L. monocytogenes	4096	8196	2	2048	2048	1	256	512	2	1	2	2
K. pneumoniae	4096	8196	2	256	512	2	128	256	2	4	8	2

[a]The microbroth dilution procedure was used to incubate the cell culture and ascertain the MIC value. In accordance with the OD_{600} values, the MIC value was chosen.

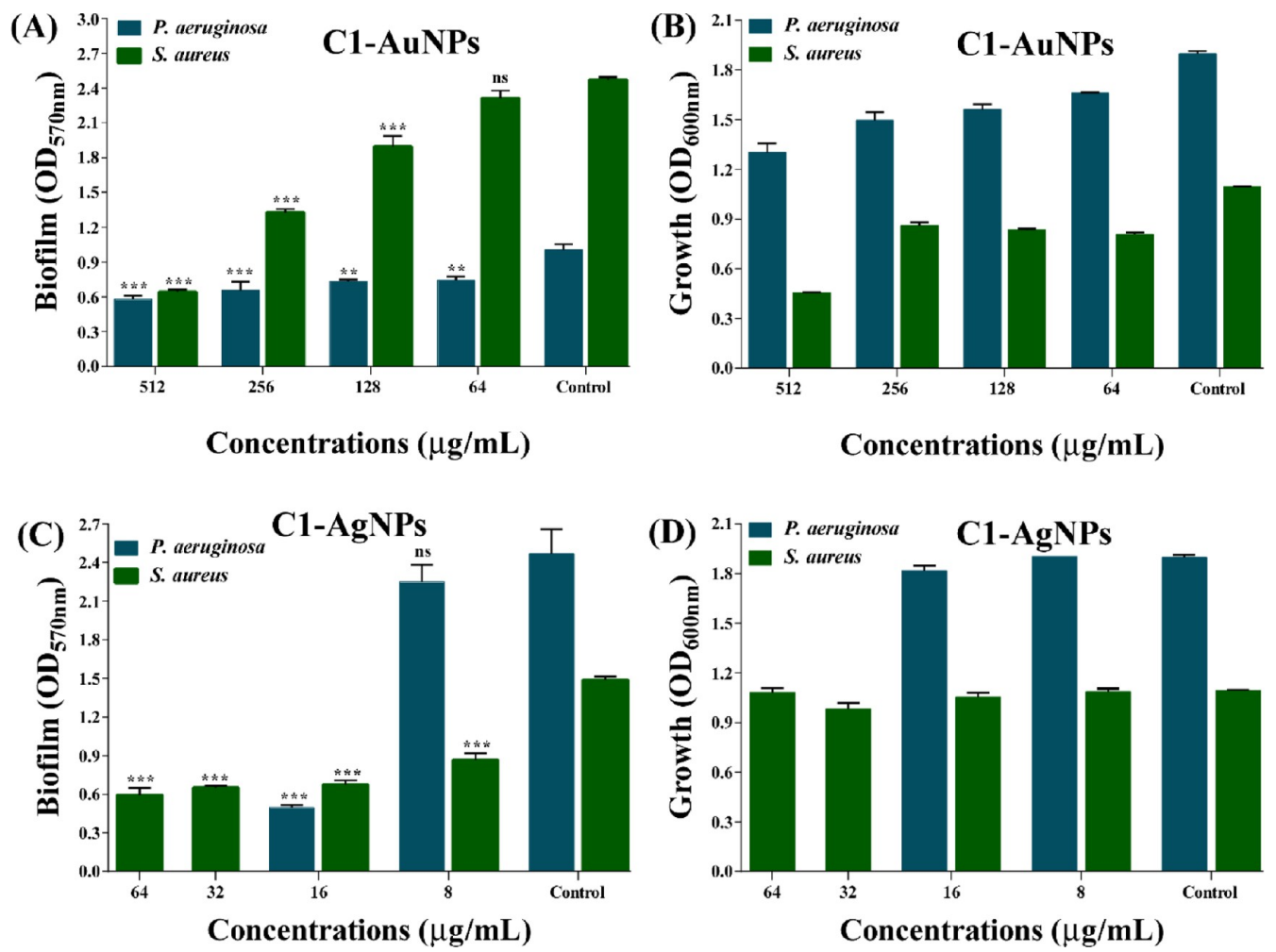

Figure 7. Initial stage biofilm inhibition by C1-AuNPs and C1-AgNPs towards *P. aeruginosa* and *S. aureus*. (A) *P. aeruginosa* and *S. aureus* biofilm inhibition by C1-AuNPs, (B) growth of *P. aeruginosa* and *S. aureus* treated with sub-MIC of C1-AuNPs, (C) *P. aeruginosa* and *S. aureus* biofilm inhibition by C1-AgNPs, and (D) growth of *P. aeruginosa* and *S. aureus* treated with C1-AgNPs. *** and ** denote significance at $p < 0.0001$ and $p < 0.01$, respectively, whereas ns denotes nonsignificance.

bacterial pathogens based on the ratio of MBC/MIC (equal to 1 or 2).

Inhibition of Initial Stage Biofilm Formation by C1-AuNPs and C1-AgNPs. The sub-MIC doses of C1-AuNPs and C1-AgNPs were used to test the early-stage biofilm inhibition (Figure 7). The biofilm inhibition data demonstrate that C1-AuNPs exhibited the greatest inhibition (42.43%) against *P. aeruginosa* at 512 μg/mL concentration (Figure 7A). Similarly, the highest suppression (73.97%) of the *S. aureus* biofilm by C1-AuNPs was determined to occur at 512 μg/mL. (Figure 7A). Furthermore, compared to *P. aeruginosa* biofilm, *S. aureus* biofilm inhibition by C1-AuNPs was concentration-dependent. The OD_{600} measurement was carried out to verify that C1-AuNPs had no inhibitory impact on *P. aeruginosa* and

https://doi.org/10.1021/acsomega.2c06789
ACS Omega 2023, 8, 9873−9888

S. aureus cell growth at the tested sub-MIC values. The results reveal that there was no inhibition of cell growth, suggesting that 100% of the cells are free to form a biofilm (Figure 7B). The biofilm inhibitory impact of C1-AgNPs on *P. aeruginosa* and *S. aureus* was also investigated at the sub-MIC level. According to the data (Figure 7C), both have strong biofilm inhibition effects. At a concentration of 16 μg/mL, C1-AuNPs inhibited *P. aeruginosa* biofilms by 79.88%. Similarly, at concentrations of 64 μg/mL, the maximal biofilm inhibition of *S. aureus* by C1-AgNPs was determined to be 60.06% (Figure 7C). The sub-MIC concentration of C1-AgNPs had no inhibitory effects on the growth of *P. aeruginosa* and *S. aureus* cells (Figure 7D). There was no inhibition of cell growth at sub-MIC levels, suggesting that there were enough cells in the assay to produce 100% biofilm.

The SEM image shows the presence of *P. aeruginosa* and *S. aureus* biofilm architecture after treatment with C1-AuNPs and C1-AgNPs at sub-MIC levels (Figure 8). The C1-AuNP-

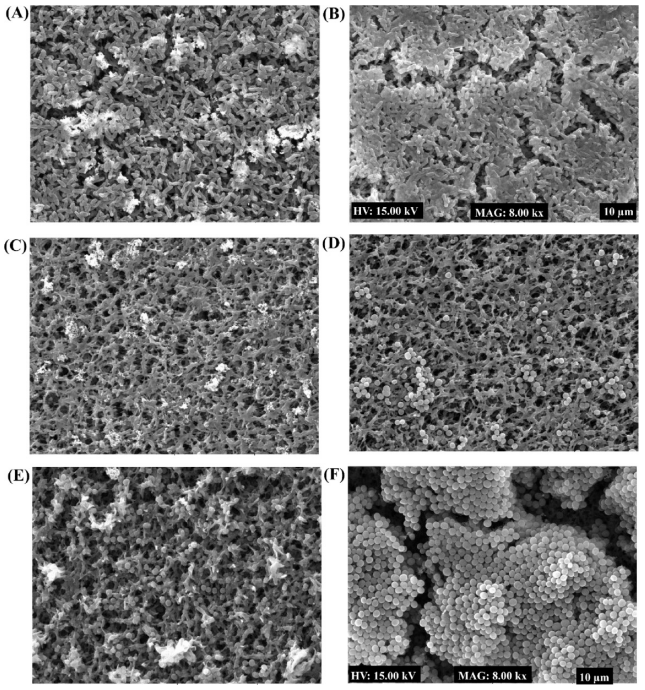

Figure 8. (A) SEM image of *P. aeruginosa* biofilms treated with C1-AuNPs, (B) SEM image of *P. aeruginosa* biofilms (control), (C) SEM image of *P. aeruginosa* biofilms treated with C1-AgNPs, (D) SEM image of *S. aureus* biofilms treated with C1-AuNPs, (E) SEM image of *S. aureus* biofilms treated with C1-AgNPs, and (F) SEM image of *S. aureus* (control).

treated cells have a slight reduction in surface attachment compared to the control cells' dense biofilm architecture (Figure 8A,B). There are almost no cells at the surface attachment in the case of C1-AgNPs treatment (Figure 8C). The biofilm architecture of *S. aureus* treated with sub-MIC C1-AuNPs was observed to have a significant reduction in surface attachment when compared to control cells (Figure 8D). Similarly, C1-AgNP-treated aureus cells exhibit the greatest reduction on the surface attached to the nylon membrane (Figure 8E) when compared to the control (Figure 8F). Based on the examination of the biofilm architecture, it was concluded that the sub-MIC of these NPs had strong biofilm inhibition of *P. aeruginosa* and *S. aureus*.

Dispersal of the Established Mature Biofilm by C1-AuNPs and C1-AgNPs. The dispersing impact of C1-AuNPs and C1-AgNPs on the established mature biofilm was also investigated using concentrations above the MIC, MIC, and sub-MIC. Although no concentration-dependent eradication was seen, both NPs were found to have strong biofilm eradication effects against *S. aureus* and *P. aeruginosa* (Figure 9A,B). The eradication of mature biofilm of *S. aureus* by C1-AuNPs at the abovementioned MIC concentration (2048 μg/mL) was determined to be 69.49% (Figure 9A), whereas 70.48% eradication was observed at the abovementioned MIC value (256 μg/mL) of C1-AgNPs (Figure 9A). Similarly, the MIC doses of C1-AuNPs (1024 μg/mL) and C1-AgNPs (128 μg/mL) were shown to be exhibits 58.48 and 50.67% eradication of mature biofilm, respectively (Figure 9A). The dispersal of mature *P. aeruginosa* biofilm by C1-AuNPs and C1-AgNPs was likewise found to be significant at various doses (Figure 9B). At the abovementioned MIC value of 2048 μg/mL, the maximal removal of *P. aeruginosa* mature biofilm by C1-AuNPs was reported to be 55.35% (Figure 9B). However, the eradication impact of C1-AuNPs was found to be 43.66% at the MIC level (1024 μg/mL), the eradication effect of C1-AgNPs was found to be 47.18% at the abovementioned MIC values (64 μg/mL) and 45.38% at the MIC level (32 μg/mL). It was observed that at the abovementioned MIC and MIC levels, both C1-AuNPs and C1-AgNPs exhibited the highest eradication effectiveness when compared to sub-MIC values.

Antimotiliy Effect of C1-AuNPs and C1-AgNPs. The sub-MIC values of these NPs have also been tested for the inhibition of several types of motilities in *P. aeruginosa* (Figure 10). *P. aeruginosa* swarming motility was significantly inhibited at the tested concentrations of C1-AuNPs and C1-AgNPs (Figure 10A,B) compared to the control (motility in the absence of NPs) (Figure 10C). The percentage of swarming motility inhibition in the presence of C1-AuNPs (256 μg/mL) and C1-AgNPs (16 μg/mL) was determined to be 78.95 and 88.02%, respectively (Figure 10D). Similarly, C1-AuNPs and C1-AgNPs significantly inhibited swimming motility (Figure 10E,F) as compared to the control (Figure 10G). Swimming motility inhibition by C1-AuNPs (256 μg/mL) and C1-AgNPs (16 μg/mL) was determined to be 66.17 and 85.29%, respectively (Figure 10H). In comparison to the control (Figure 10K), C1-AuNPs and C1-AgNPs inhibited pilli-mediated twitching motility (Figure 10I,J). The percentages of twitching motility inhibition by C1-AuNPs (256 μg/mL) and C1-AgNPs (8 μg/mL) were determined to be 40.27 and 77.77% (Figure 10L), respectively.

Inhibition of Diverse Virulence Properties by C1-AuNPs and C1-AgNPs. The effects of C1-AuNPs and C1-AgNPs on various virulence factors in *P. aeruginosa* and *S. aureus* have been studied. In the instance of *P. aeruginosa*, the sub-MIC values of C1-AuNPs and C1-AgNPs were used to assess the inhibition of protease activity, hemolytic activity, and the inhibition in pyocyanin and pyoverdine levels. However, in the case of *S. aureus*, we solely investigated the antihemolytic action of these NPs. The maximum inhibition of the hemolytic effects of C1-AuNPs and C1-AgNPs on *P. aeruginosa* was reported to be 31.37% (Figure 11A) and 45.88% (Figure 11B) at doses of 512 and 16 μg/mL, respectively. Similarly, both C1-AgNPs and C1-AuNPs significantly inhibited the hemolysis of *S. aureus*. The percentage of inhibition of *S. aureus* hemolytic activity by C1-AuNPs and C1-AgNPs was determined to be 49.67% (Figure 11C) and 91.79% (Figure 11D) at the

https://doi.org/10.1021/acsomega.2c06789
ACS Omega 2023, 8, 9873−9888

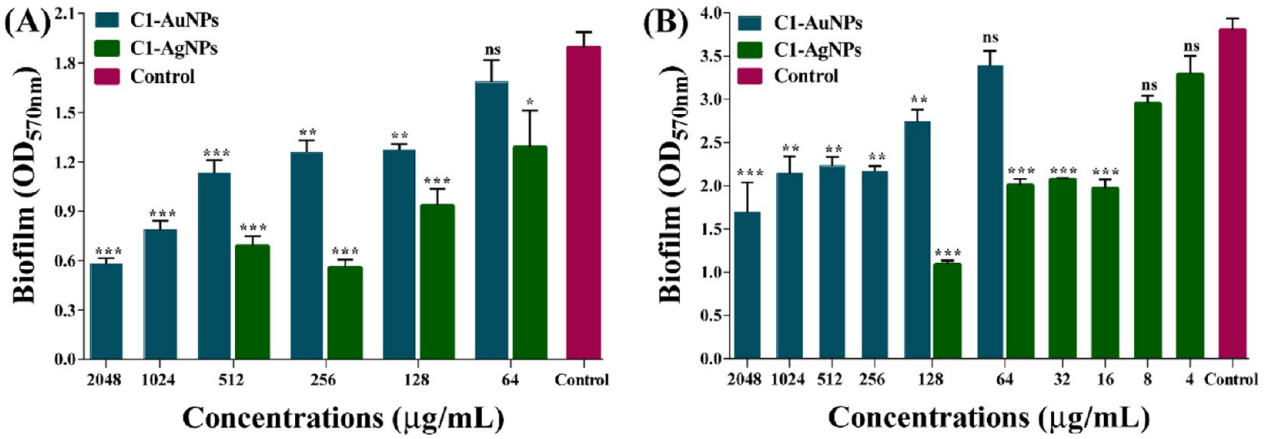

Figure 9. Dispersal of established mature biofilm of *P. aeruginosa* and *S. aureus* by C1-AuNPs and C1-AgNPs. (A) Dispersal of mature biofilm of *S. aureus* by C1-AuNPs and C1-AgNPs and (B) dispersal of mature biofilm of *P. aeruginosa* mature biofilm by C1-AuNPs and C1-AgNPs. ***, **, and * denote significance at $p < 0.0001$, $p < 0.01$, and $p < 0.05$, respectively, and ns denotes nonsignificance.

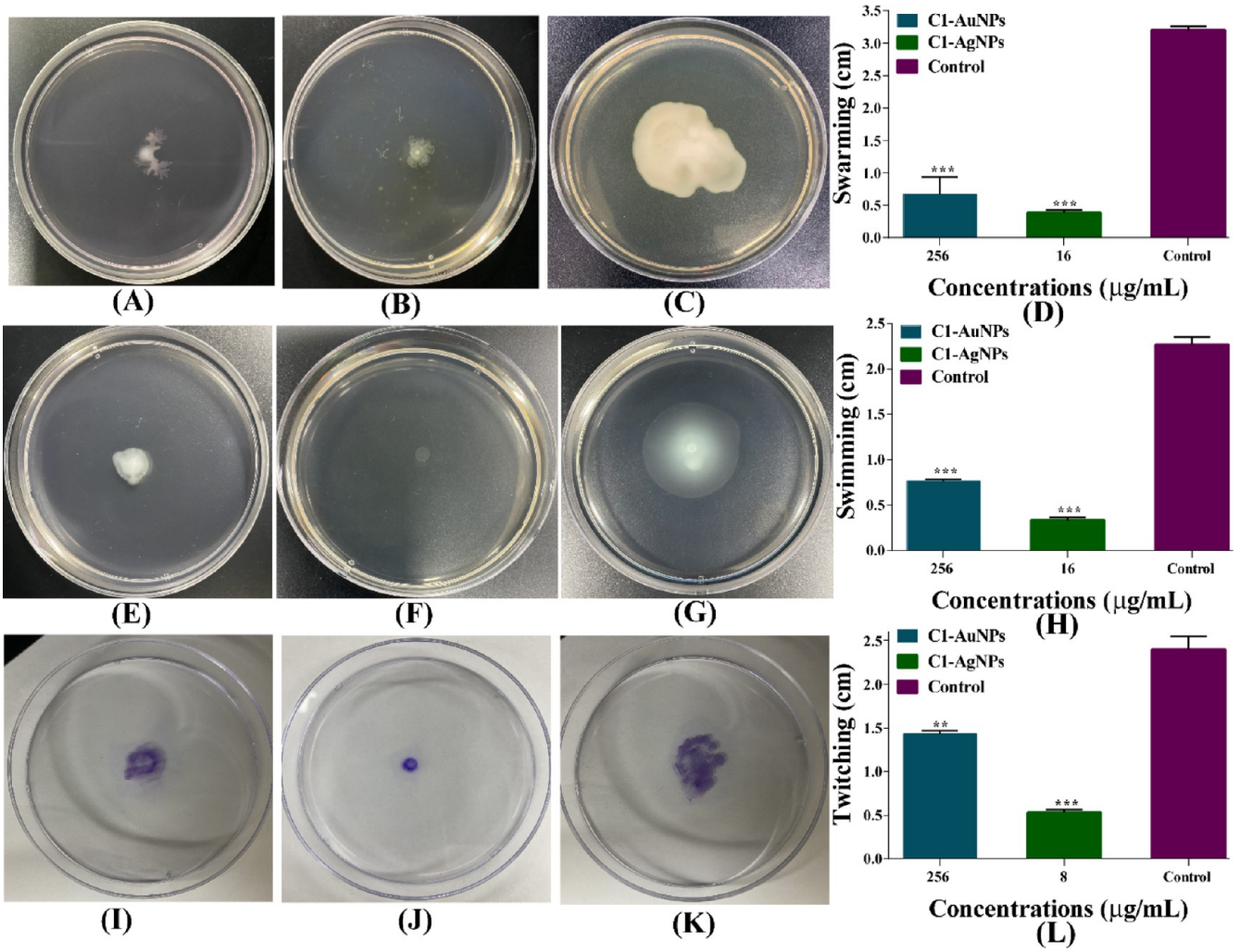

Figure 10. (A) Reduction of swarming motility by C1-AuNPs, (B) reduction of swarming motility by C1-AgNPs, (C) swarming of control cells, (D) bar diagram showing the inhibition of swarming motility by C1-AuNPs and C1-AgNPs, (E) reduction of swimming motility by C1-AuNPs, (F) reduction of swimming motility by C1-AgNPs, (G) swimming of control cells, (H) bar diagram showing inhibition of swimming motility by C1-AuNPs and C1-AgNPs, (I) reduction of twitching motility by C1-AuNPs, (J) reduction of twitching motility by C1-AgNPs, (K) twitching of control cells, and (L) bar diagram showing inhibition of twitching motility by C1-AuNPs and C1-AgNPs. *** and ** denote significance at $p < 0.0001$ and $p < 0.01$, respectively.

https://doi.org/10.1021/acsomega.2c06789
ACS Omega 2023, 8, 9873−9888

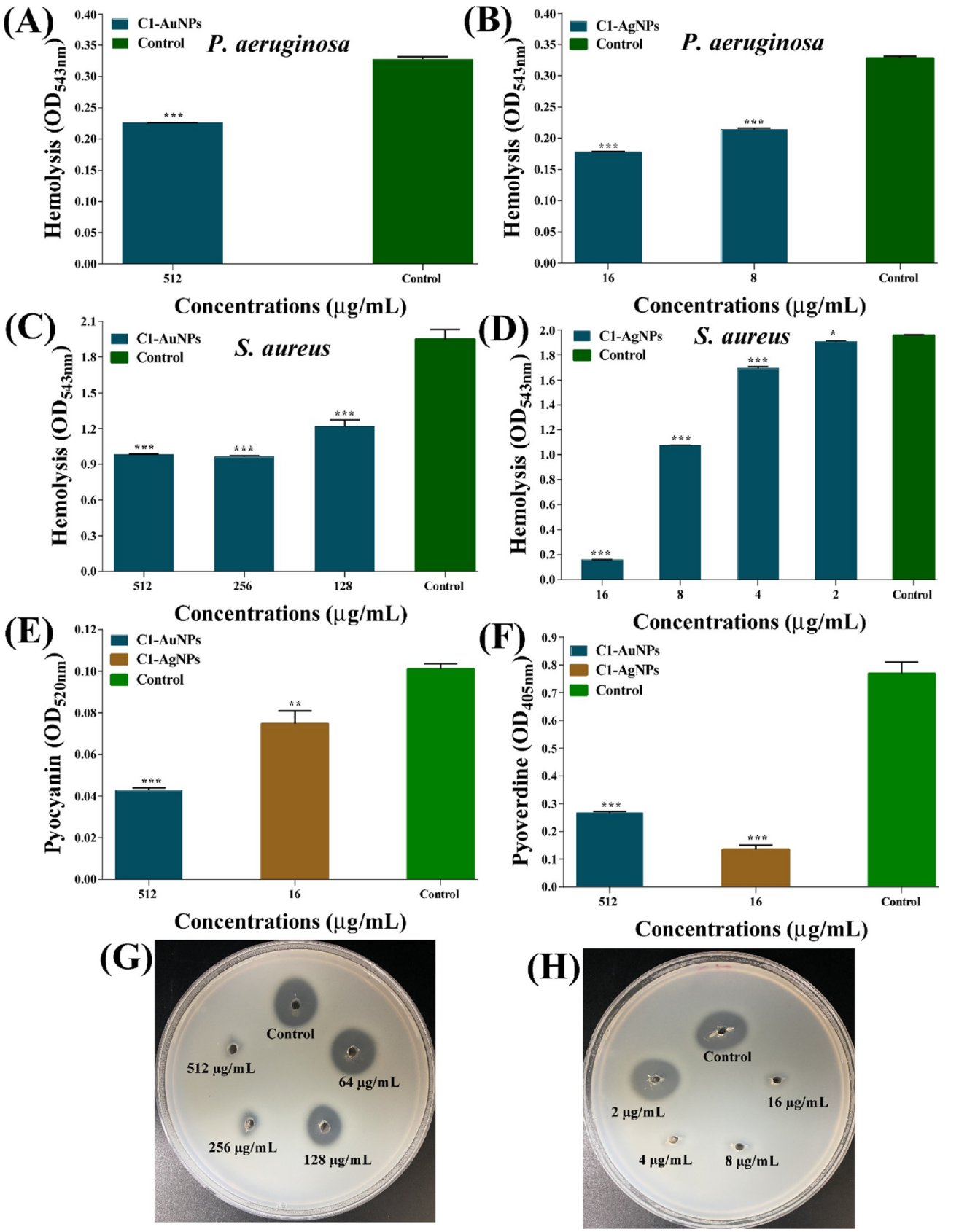

Figure 11. (A) Inhibition of *P. aeruginosa* hemolytic activity by C1-AuNPs, (B) inhibition of *P. aeruginosa* hemolytic activity by C1-AgNPs, (C) inhibition of *S. aureus* hemolytic activity by C1-AuNPs, (D) inhibition of *S. aureus* hemolytic activity by C1-AgNPs, (E) pyocyanin inhibition by C1-AuNPs and C1-AgNPs in *P. aeruginosa*, (F) pyoverdine inhibition by C1-AuNPs and C1-AgNPs production in *P. aeruginosa*, (G) protease inhibition by C1-AuNPs in *P. aeruginosa*, and (H) protease inhibition by C1-AgNPs in *P. aeruginosa*. *** and ** denote significance at $p < 0.0001$ and $p < 0.01$, respectively.

https://doi.org/10.1021/acsomega.2c06789
ACS Omega 2023, 8, 9873−9888

concentrations of 512 and 16 μg/mL, respectively. *P. aeruginosa* pyocyanin production was considerably reduced when cells were treated with sub-MIC doses of C1-AuNPs and C1-AgNPs (Figure 11E). The maximum inhibition of pyocyanin in the presence of C1-AuNPs and C1-AgNPs was recorded at 57.75% (at 512 μg/mL) and 26.07% (at 16 μg/mL), respectively (Figure 11E). The inhibition of the siderophore pyoverdine by these NPs was shown to be effective in *P. aeruginosa* (Figure 11F). In the presence of C1-AuNPs at 512 μg/mL, the highest (65.26%) amount of pyoverdine was inhibited. Pyoverdine inhibition was reported to be 82.45% under the influence of C1-AgNPs at 16 μg/mL. The inhibition of *P. aeruginosa* protease enzyme activity was found to be significant, as evidenced by the inhibition of the development of a clear zone around the hole on skim-milk agar plates. There was a negligible zone of clearance in the cell supernatant obtained from cells treated with 512 μg/mL doses of C1-AuNPs (Figure 11G). Similarly, C1-AgNPs were reported to have strong inhibitory effects at 16, 8, and 4 μg/mL. (Figure 11H). In comparison to C1-AgNPs, the protease activity of C1-AuNPs was found to be concentration-dependent. The results of this investigation indicate that, in addition to their biofilm inhibitory action, these NPs are effective against the virulence features of bacterial pathogens.

Presence of Different Types of Secondary Metabolites in the LAB Supernatant. The Gas chromatograph-Mass Spectroscopy (GC−MS) analysis reveals the presence of many secondary metabolites produced by strain C1, as shown in the Supporting Information (Table S1). Several major and minor peaks were observed in the GC chromatogram (Figure S1), and these peaks were searched from the NIST library. Table S1 summarizes the discovered compounds, together with their retention time and composition %. Furthermore, the biological roles of these compounds were discovered to have previously been reported, with various types such as antioxidant, antibacterial, anti-inflammatory, and anticancer properties, which are also summarized in Table S1. Maltol, 2,3-dihydro-3,5-dihydroxy-6-methyl-4*H*-pyran-4-one, and ergotamine are all antioxidant metabolites. The presence of these antioxidants indicates that the prepared supernatant from the C1 strain efficiently reduced ionic metals into gold and silver nanoparticles. Similarly, several antimicrobial compounds identified in GC−MS analysis (Table S1) indicate that the supernatant from strain C1 has antibacterial activity against several microbial pathogens. Based on the identified metabolites with antioxidant and antibacterial activity, the LAB strain C1 is a viable candidate for synthesizing metallic nanoparticles and testing their antimicrobial capabilities.

DISCUSSION

With the rising AMR traits in microbial pathogens, the search for potential antimicrobial drugs is always in high demand. The approaches to control bacteria pathogens include physical, chemical, and biological methods.[32,33] The formation of biofilm by bacteria has become one of the most challenging issues in infection treatment because EPS restricts drug entry.[34] Nanotechnology has emerged as a prominent field for the production of nanomaterials for use in the pharmaceutical, agricultural, food, biomedical, and clinical sectors lately.[35,36] Employing green synthesis of nanoparticles has been one of the more promising ways, with various benefits over chemical and physical methods.[37] Furthermore, the use of materials derived from probiotics provides additional benefits for synthesizing nanoparticles with improved compatibility and acceptance due to the numerous health benefits of probiotics.[38] We isolated 15 LAB isolates from the Kimchi sample to synthesize metallic nanoparticles, such as AuNPs and AgNPs, as a probiotic extract. Among these, *Lactiplantibacillus* sp. strain C1, with possible antioxidant activity, was identified. Table S1 summarizes the identified metabolites from the supernatant of *Lactiplantibacillus* sp. strain C1 that show antioxidant and antimicrobial activity.[39−41] Thus, the presence of the antimicrobial and antioxidant component in the supernatant of strain C1 confirms its suitability for the synthesis of AuNPs and AgNPs. Furthermore, the antibacterial activity of the prepared C1 supernatant against bacterial pathogens in the current study provides proof of the presence of the antimicrobial component in the supernatant. As previously reported, the obtained supernatant from LAB serves as an excellent reducing agent for the conversion of metallic ions into nanoparticles.[42−45]

The AuNPs and AgNPs were synthesized using the supernatant from strain C1. The confirmation of the synthesized AuNPs was made based on a visual inspection of the color change from yellow to red wine, whereas for AgNPs, the formation of precipitates was considered confirmation.[46,47] Furthermore, the appearance of particular absorption peaks at 560 nm and 400 nm was considered evidence for the synthesis of C1-AuNPs and C1-AgNPs. These observed absorption peaks in C1-AuNPs and C1-AgNPs are in close accord with previously produced NPs utilizing natural materials.[47−49] The spherical form of the C1-AuNPs and C1-AgNPs is consistent with nanoparticles previously synthesized utilizing microbial extracts.[43,50,51] Similarly, the sizes of C1-AuNPs and C1-AgNPs were comparable to previously reported green synthesized AuNPs and AgNPs.[52] The high negative values of the zeta potential of C1-AuNPs and C1-AgNPs, such as −23.29 ± 1.17 and −30.57 ± 0.29 mV, indicate stable NPs and are consistent with prior findings.[52]

The biofilm inhibition of *P. aeruginosa* and *S. aureus* by C1-AuNPs and C1-AgNPs at their sub-MIC levels was shown to be different. *P. aeruginosa* and *S. aureus* biofilm inhibition by C1-AuNPs was observed to occur at a higher concentration than inhibition by C1-AgNPs. Maximum biofilm inhibition of these pathogens by C1-AgNPs was observed to occur at a four-fold lower concentration of C1-AgNPs with a comparable rate of inhibition. The findings suggest that C1-AgNPs are more effective antibiofilms than C1-AuNPs. Previous research has shown that AuNPs synthesized from various natural products require the same concentration as C1-AuNPs to inhibit biofilm formation.[46] The required biofilm inhibitory concentration of C1-AgNPs is also consistent with prior observations in which a low concentration of AgNPs produced from other natural products is also required.[53,54] The requirement of high concentrations (> MIC and MIC) of C1-AuNPs and C1-AgNPs for maximal eradication of established mature biofilms suggests that mature biofilms have a thick EPS matrix that requires a high concentration to disperse.[55,56] Former research has also shown that a very high concentration of AuNPs is necessary to eradicate mature biofilm by AuNPs.[46,57] Based on the findings of this work, it is concluded that these NPs can be used as a possible agent to inhibit biofilm development on surfaces (biotic and abiotic) where biofilm formation is common.[10,11]

In addition to managing the biofilm, attenuation of the virulence factors produced by *P. aeruginosa* and *S. aureus* has

https://doi.org/10.1021/acsomega.2c06789
ACS Omega 2023, 8, 9873−9888

been postulated as another method of controlling their infection.[58−60] C1-AuNPs and C1-AgNPs both inhibit *P. aeruginosa* flagella-mediated and pilli-mediated motility at sub-MIC levels. The concentration necessary for maximum inhibition of swarming, swimming, and twitching motilities by these NPs was similar to the concentration required for maximum inhibition of biofilms. The suppression of several types of motilities by these NPs is consistent with previously described biogenic-based synthesized NPs.[46,61] Inhibiting motilities in *P. aeruginosa* will assist in controlling the formation of initial-stage biofilms and cell dispersal during mature biofilm dispersal.[62] *P. aeruginosa* virulence properties (e.g., pyocyanin and pyoverdine production and hemolytic and protease activity) and hemolytic activity of *S. aureus* were significantly inhibited by the same dose that inhibited biofilm and motility properties. Previous research on the attenuation of these various virulence properties by C1-AuNPs and C1-AgNPs supports the current finding.[46,63]

CONCLUSIONS

The present study includes isolating and identifying LAB strains from Kimchi samples using a molecular technique. The strain C1, also known as *Lactipalntibacillus* sp. strain C1, was selected as the best antioxidant bacterium to synthesize two types of metallic nanoparticles, C1-AuNPs and C1-AgNPs. The synthesized C1-AuNPs and C1-AgNPs have been fully characterized as spherical in shape, crystalline in nature, and highly stable using a variety of instrumental techniques such as UV−visible absorption spectroscopy, FTIR, FE-TEM, DLS, and XRD. Furthermore, GC−MS analysis of the C1 supernatant reveals the presence of a variety of organic secondary metabolites. These metabolites have previously been found to exhibit various biological actions such as anticancer, antioxidant, antiviral, antibacterial, and antifungal properties. The NPs were physiochemically analyzed utilizing several types of equipment. Antibacterial properties such as antibiofilm and antivirulence features of these NPs were examined against human bacterial pathogens. C1-AuNPs and C1-AgNPs significantly inhibited the initial stage biofilm of *P. aeruginosa* and *S. aureus*, which was corroborated by studying the biofilm architecture using SEM. When exposed to the MIC and sub-MIC of C1-AuNPs and C1-AgNPs, the mature biofilms of *P. aeruginosa* and *S. aureus* were shown to be substantially eradicated. *P. aeruginosa* virulence properties such as pyocyanin, pyoverdine production, protease action, and hemolytic action were all inhibited by sub-MIC C1-AuNPs and C1-AgNPs. After treatment with sub-MICs of both NPs, *S. aureus* hemolytic activity was dramatically reduced. C1-AuNPs and C1-AgNPs also reduced the QS-mediated distinct forms of motility of *P. aeruginosa*. The overall study concluded that probiotic-based synthesized NPs would be prospective candidates for reducing the initial-stage biofilm, removing the mature biofilm, and disarming numerous virulence properties of human pathogenic bacteria. Since the present study revealed phenotypic-based prevention of biofilm and virulence features, subsequent analyses of the gene expression of relevant genes are required to elucidate the molecular mechanisms.

MATERIALS AND METHODS

Chemicals, Microbial Strains, Culture Media, and Growth Conditions. Gold(III) chloride trihydrate (CAS# 16961-25-4; 99% pure) and silver nitrate (CAS# 7761-88-8; ≥99.0% pure) were purchased from Sigma-Aldrich Co. (St. Louis, MO, USA). The bacterial strains, essentially *P. aeruginosa* PAO1 (KCTC 1637), *E. coli* (KCTC1682), *S. aureus* (KCTC 1916), and *L. monocytogenes* (KCTC3569), were purchased from the Korean Collection for Type Cultures (KCTC, Daejeon, Korea). Similarly, the bacteria *S. mutans* (KCCM 40105) was obtained from the Korean Culture Center of Microorganisms (KCCM; Seodaemun-gu, Seoul). In contrast, *K. pneumoniae* (ATCC 4352) was received from the American Type Culture Collection (ATCC). Bacterial strain. such as *E. coli*, *P. aeruginosa*, *S. aureus*, and *L. monocytogenes*, were grown in Tryptic soy broth (TSB) (Difco Lacboratory Inc., Detroit, MI, USA). Brain Heart Infusion broth (BHI) (Difco Laboratory Inc., Detroit, MI, USA) was used for *S. mutans*. In deMaan Rogosa Sharpe Medium, LAB strain C1 was checked for growth and subculturing (MRS; Difco Lacboratory Inc., Detroit, MI, USA). The growth study of these microbes and other biological experiments were carried out at 37 °C.

Lactic Acid Bacteria Isolation and Identification. The previously reported procedure was used to isolate LAB from the Kimchi sample.[64] Kimchi (25 gm) was homogenized by diluting (10^{-10}) in phosphate-buffered saline (PBS) (0.1 M: pH 7.2). The diluted solution was spread plated on MRS agar plates with 0.002% (w/v) Bromocresol purple (Duksan Pure Chemical Co., Ltd.) and incubated at 37 °C for 24 h. Based on the presence of a yellow tint surrounding the colony, which was due to the production of organic acid by LAB, the pure LAB colony was separated from the agar plate. The pure bacterial colonies were further screened as potential antioxidant candidates. For molecular examination, 16S rRNA gene sequencing was targeted to identify potential antioxidants showing bacterial colonies.[64,65] The 16S rRNA gene region was determined by the Bionics sequencing service (SEOUL, Korea) using 27F (5′-AGAGTTTGATCCTGGCTCAG-3′) and 1492R (5′-GTTACCTGTTACGACTT-3′) primer pairs. The 16S rRNA gene sequence retrieved was blast-searched against the EzBioCloud 16S database. The sequence alignment of the 16S rRNA gene of strain C1 with the types of strains available from the EzBioCloud 16S database was performed. The phylogenetic tree was created using MEGA 11, a neighbor-joining algorithm, and a distance estimation method.[66]

Preparation of Supernatant from Cell Culture of Strain C1. Bacterial strain C1 was grown in an MRS medium for 24 h at 37 °C, and when cell growth reached ∼9 log cfu/mL, the cell cultures were centrifuged (10 000*g* for 20 min) at 4 °C. Using a freeze-dryer (FD8518, ilShinBiobase Co. Ltd., Yangju-si, Korea), the recovered filter-sterilized supernatant was freeze-dried into powder form. The sterilized supernatant was employed for three separate purposes: (1) testing antibacterial activity, (2) synthesis of metallic nanoparticles, and (3) secondary metabolite profiling from LAB strain C1 cell culture.

Synthesis of Metallic Nanoparticles. The LAB supernatant was used to synthesize two types of metallic nanoparticles, gold (C1-AuNPs) and silver nanoparticles (C1-AgNPs), as previously described.[46] The alkaline pH of the LAB supernatant was adjusted with 0.1 N NaOH for nanoparticle synthesis. The C1-AuNPs were synthesized by dissolving 1 mM gold (III) chloride trihydrate ($HAuCl_4 \cdot 3H_2O$) in 200 mL of deionized water and setting the pH to 9. The solution was regularly stirred, and the temperature was

https://doi.org/10.1021/acsomega.2c06789
ACS Omega 2023, 8, 9873−9888

maintained at 60 °C. Dropwise LAB supernatant (3 mL) was added to the solution, and continuous stirring at 60 °C was allowed. The color change from yellow to dark-red wine indicates the formation of AuNPs. Furthermore, the appearance of the AuNPs' particular absorption peak was examined by scanning the spectra (in the range of 200−700 nm) using a microplate reader (BioTek, Winooski, VT, USA). After freezing at −70 °C for 2 h, the sample was immediately placed in the freeze dryer to lyophilize the AuNPs in powder form. The silver nanoparticles were synthesized using a somewhat different method (AgNPs). Silver nitrate (2 mM) was dissolved in 200 mL of deionized water. The prepared supernatant (3 mL) from strain C1 was added to the bottle, covered with aluminum foil to keep it dark, and maintained at 37 °C overnight. Furthermore, an increase in the absorption peak at a specific wavelength suggests the formation of AgNPs. To get the pellet, the sample was centrifuged at 4 °C for 30 min at 13000 rpm. The pellet was cleansed with deionized water before being freeze-dried to powder.

Analysis of Secondary Metabolites Produced by Strain C1. The identification of metabolites present in the LAB supernatant was accomplished using GC−MS analysis.[26] The GC−MS equipment (Agilent Technologies 7890A-5975C) was used to examine the metabolites in the supernatant. The helium gas was used as the carrier with a 1.0 mL/min flow rate. The sample (1.0 1.0 μL) was injected into the GC−MS machine for 1 min with a split flow delay and resolved using a DB-5MS column (Agilent Technologies, Palo Alto, CA, USA). The GC's inlet, interface, and ion sources were programmed at 250, 250, and 230 °C, respectively. The start and end temperatures of the oven were 50 and 230 °C, with a 5 °C/min rate, followed by 2 min at a constant temperature. The mass spectra of each compound in m/z were analyzed from 50 to 550 at 70 eV. Each peak in the GC chromatogram was analyzed, and the metabolites were identified using the chemical compound database accessible in the National Institute of Standards and Technology database.

Instrumental Characterization of the Synthesized Nanoparticles. The detailed characterization of synthesized AuNPs and AgNPs was carried out in line with the previously described procedures.[67] The initial characterization of these NPs was performed by scanning UV−vis absorption spectra from 200 to 700 nm with a microplate reader (BioTek, Winooski, VT, USA) to check for a specific absorption peak. FETEM (JEM-F200, JEOL, Japan) was used to examine the shape and morphology of these nanoparticles. The ionic interaction in the synthesized NPs was verified by scanning the spectra with FTIR (JASCO (FT-4100), Tokyo, Japan). The frequencies used in the FTIR ranged from 400 to 4000 cm^{-1}. Using a particle analyzer, the Litesizer 500 (Anton Paar, GmbH), the average size and zeta potential of AuNPs and AgNPs were determined. The elemental mapping and EDS of these NPs were performed on the same FE-TEM device that was used to check the morphology. The XRD (Rigaku (Japan), Ultima IV) equipment was employed to determine the crystalline nature of C1-AuNPs and C1-AgNPs.

Testing of the Antimicrobial Efficacy of the Supernatant and Nanoparticles. The powdered forms of C1 supernatant, C1-AuNPs, and C1-AgNPs were utilized to test their antibacterial properties on various microbial pathogens, as shown in Table 1. The procedure for determining the minimum inhibitory concentration (MIC) values was followed as previously reported.[68] In brief, the seed culture of these microorganisms was diluted in their respective growth media to attain the requisite OD_{600} value of 0.05. These cell cultures in the 96-well microplate were incubated with various NP concentrations (ranging from 4 to 2048 μg/mL). However, cell-free supernatant from the C1 strain was added to the 96-well microplate in steps ranging from 128 to 4086 μg/mL. The cell culture and NPs added to the microplate were incubated for 24 h at 37 °C. After incubation, the OD at 600 nm of the growing cells was evaluated with a microtiter plate reader. The MIC values of each NP were calculated based on the inhibition of cell growth (>90%) at various doses. Furthermore, the visual inspection of cell growth inhibition was also used to calculate the MIC values. The MBC of C1-AuNPs, C1-AgNPs, C1 supernatant, and tetracycline (as positive control) towards microbial pathogens has been determined as described previously.[69] The MBC experiment was carried out by incubating the microbial cells in the 96-well microtiter plate with NPs at the ≥MIC concentration. On the TSA, the NP-treated cell culture (100 μL) was spread-plated. The MBC endpoint of the tested concentration was noted when there were no visible colonies on the agar plate. The bactericidal effect was determined using the MBC/MIC ratio as previously described.[70]

Biofilm Assays. The early-stage biofilm inhibition by C1-AuNPs and C1-AgNPs was evaluated using the previously described approach.[46] The sub-MIC values of C1-AuNPs and C1-AgNPs were used to evaluate biofilm inhibition against *P. aeruginosa* and *S. aureus*. 300 μL of microbial cell culture with an OD_{600} value of 0.05 was put in a 96-well microplate with different concentrations of C1-AuNPs and C1-AgNPs (4−2048 μg/mL). The microplate was kept for incubation for 24 h at 37 °C. Total cell growth in the presence of NPs was measured using a microplate reader set to 600 nm. The planktonic cells were discarded from each well, and the adherent cells were rinsed three times with distilled water. Crystal violet was applied to the biofilm cells for 20 min, and the stained cells were rinsed thrice with distilled water. The dye-stained cells were dissolved in 95% concentrated ethanol, and the biofilm measurement was done at 570 nm.

Similarly, the dispersing impact of these NPs on the pathogens' established mature biofilm was investigated utilizing the abovementioned MIC, MIC, and sub-MIC values of these NPs.[46] The mature biofilm of pathogens was formed by growing cell culture (OD_{600} = 0.05) in a 96-well microplate. The plate was incubated at 37 °C for 24 h to allow for the establishment of a mature biofilm. The planktonic cells were discarded, while the adhering ones were rinsed three times with TSB. The mature biofilm was treated with varied dosages of NPs (ranging from 64 to 2048 μg/mL). The microplate was then incubated at 37 °C for another 24 h. The regrown plankton was removed, and the dye-stained biofilm was quantified by measuring the OD at 570 nm.

Visualization of the Biofilm Architecture Using SEM. The antibiofilm activity of C1-AuNPs and C1-AgNPs was further validated by analyzing the structure of the biofilm through SEM, as previously described.[46] *P. aeruginosa* and *S. aureus* cell cultures (OD_{600} = 0.05) were put in a 24-well microplate with a nylon membrane size of 0.5 × 0.5 cm. These wells were then incubated for 24 h at 37 °C with sub-MIC values of C1-AuNPs and C1-AgNPs. A control group was a well that had not been treated with NPs. The cells were fixed directly in glutaraldehyde and formaldehyde at 4 °C for 12 h.

https://doi.org/10.1021/acsomega.2c06789
ACS Omega 2023, 8, 9873−9888

The biofilm cells were thoroughly washed three times in PBS to remove planktonic cells altogether. The biofilm cells were dehydrated by incubating them in ethyl alcohol concentrations ranging from 50 to 95%. A freeze-drier was used to dry the biofilm cells completely, and a picture of the biofilm cells was captured using SEM TESCAN (Vega II LSU; Czech).

Analysis of the Virulence Properties. The effect of C1-AuNPs and C1-AgNPs on *P. aeruginosa* virulence features such as pyoverdine, pyocyanin, protease activity, and hemolytic activity was studied as previously described.[71] In the instance of *S. aureus*, the hemolytic activity was carried out in the presence of C1-AuNPs and C1-AgNPs. The inhibitory impact of NPs on pyocyanin formation from *P. aeruginosa* was tested by incubating several sub-MIC values of NPs with cell culture ($OD_{600} \sim 0.05$). These cells were incubated at 37 °C for 24 h. Chloroform and 0.1 N HCl were used to extract the pink pigment, and the OD at 520 nm was examined later.[72] By incubating the cell culture ($OD_{600} = 0.05$) in low salt media of sodium succinate (2%), pyoverdine synthesis from *P. aeruginosa* was evaluated in the presence of NPs by measuring the OD at 405 nm. The hemolytic activity of cells treated with NPs was tested as described earlier.[71] The NP-treated cell culture (50 μL) was mixed with 950 μL of diluted sheep red blood cells (RBCs; MBcell Ltd., Seoul, Korea) and incubated for 3 h at 37 °C. The sample was centrifuged, and the quantity of lyzed RBCs in the supernatant was detected at 534 nm. The inhibition of *P. aeruginosa* protease activity by C1-AuNPs and C1-AgNPs was tested using agar media added with 2% skim milk. The filter-sterilized supernatant obtained from the NP-treated cell culture was inserted into the hole made in the skim-milk agar plate. The clear zone surrounding the hole was observed.

Flagella-based motilities in *P. aeruginosa* (e.g., swimming and swarming) as well as pilli-mediated motilities, such as twitching, were also evaluated for C1-AuNPs and C1-AgNPs, as previously described.[71] Swarming motility is performed using Luria Bertani (LB) broth media with Bacto agar (0.5%), 0.4% glucose, and 0.4% casamino acid. In contrast, the swimming motility medium was made in LB by dissolving Bacto agar (0.3%), tryptone (1%), and NaCl (0.25%). Bacto agar (1.5%), casamino acid (0.2%), and glucose (30 mM) were used to test twitching motility. Autoclaved media were mixed with C1-AuNPs and C1-AgNPs and poured into Petri dishes. Swimming and swarming experiments were performed by placing the microbial cell culture (3 μL) in the center of the agar plate and incubating it for 24 h at 37 °C. The diameter of cells moved on the agar surface was measured. In the case of twitching, the cell culture was deposited in the Petri plates using a sterilized toothpick, followed by the pouring of twitching agar media. The solid agar media was removed in the case of twitching motility and stained with crystal violet. The diameters of the stained cells were measured and compared to the control.

Statistical Analysis. Each graph was plotted using GraphPad Prism 7.0 (GraphPad Software Inc., San Diego, CA). The experiment was statistically analyzed using a one-way ANOVA. $***p < 0.0001$, $**p < 0.01$, and $*p < 0.05$ were considered significant. The triplicate samples were taken, and the experiment was repeated three times. Furthermore, the data in the graph were presented as the mean ± standard error.

■ ASSOCIATED CONTENT

Supporting Information

The Supporting Information is available free of charge at https://pubs.acs.org/doi/10.1021/acsomega.2c06789.

GC−MS chromatogram of the supernatant obtained from the cell culture of strain C1 and GC−MS of C1 supernatant (PDF)

■ AUTHOR INFORMATION

Corresponding Authors

Fazlurrahman Khan − *Marine Integrated Biomedical Technology Center, The National Key Research Institutes in Universities, Pukyong National University, Busan 48513, Republic of Korea; Research Center for Marine Integrated Bionics Technology, Pukyong National University, Busan 48513, Republic of Korea*; Phone: +82-51-629-5832; Email: fkhan055@pknu.ac.kr; Fax: +82-51-629-5824

Young-Mog Kim − *Department of Food Science and Technology and Marine Integrated Biomedical Technology Center, The National Key Research Institutes in Universities, Pukyong National University, Busan 48513, Republic of Korea; Research Center for Marine Integrated Bionics Technology, Pukyong National University, Busan 48513, Republic of Korea*; orcid.org/0000-0002-2465-8013; Phone: +82-51-629-5832; Email: ymkim@pknu.ac.kr; Fax: +82-51-629-5824

Authors

Min-Gyun Kang − *Department of Food Science and Technology, Pukyong National University, Busan 48513, Republic of Korea*

Nazia Tabassum − *Marine Integrated Biomedical Technology Center, The National Key Research Institutes in Universities, Pukyong National University, Busan 48513, Republic of Korea; Research Center for Marine Integrated Bionics Technology, Pukyong National University, Busan 48513, Republic of Korea*

Kyung-Jin Cho − *Department of Food Science and Technology, Pukyong National University, Busan 48513, Republic of Korea*

Du-Min Jo − *Department of Food Science and Technology and Marine Integrated Biomedical Technology Center, The National Key Research Institutes in Universities, Pukyong National University, Busan 48513, Republic of Korea; Research Center for Marine Integrated Bionics Technology, Pukyong National University, Busan 48513, Republic of Korea*

Complete contact information is available at: https://pubs.acs.org/10.1021/acsomega.2c06789

Author Contributions

Credit Authorship Contribution Statement: **Min-Gyun Kang:** methodology, investigation, and data curation; **Fazlurrahman Khan:** conceptualization, supervision, methodology, investigation, data curation, and writing-original draft and editing; **Nazia Tabassum:** investigation and data curation; **Kyung-Jin Cho**: investigation and data curation; **Du-Min Jo**: investigation and data curation; and **Young-Mog Kim**: conceptualization, supervision, funding, and writing—review and editing.

Funding

This research was supported by the Basic Science Research Program through the National Research Foundation of Korea

(NRF) grant funded by the Ministry of Education (2021R1A6A1A03039211 and 2022R1A2B5B01001998). This research was also supported by the Korea Institute of Marine Science & Technology Promotion (KIMST) and funded by the Ministry of Oceans and Fisheries (20220319).

Notes

The authors declare no competing financial interest.

REFERENCES

(1) De Oliveira, D. M. P.; Forde, B. M.; Kidd, T. J.; Harris, P. N. A.; Schembri, M. A.; Beatson, S. A.; Paterson, D. L.; Walker, M. J. Antimicrobial Resistance in ESKAPE Pathogens. *Clin. Microbiol. Rev.* **2020**, *33*, No. e00181-19.

(2) Murray, C. J.; Ikuta, K. S. Global burden of bacterial antimicrobial resistance in 2019: a systematic analysis. *Lancet* **2022**, *399*, 629−655.

(3) Reygaert, W. C. An overview of the antimicrobial resistance mechanisms of bacteria. *AIMS Microbiol.* **2018**, *4*, 482−501.

(4) Peterson, E.; Kaur, P. Antibiotic Resistance Mechanisms in Bacteria: Relationships Between Resistance Determinants of Antibiotic Producers, Environmental Bacteria, and Clinical Pathogens. *Front. Microbiol.* **2018**, *9*, 2928.

(5) Szomolay, B.; Klapper, I.; Dockery, J.; Stewart, P. S. Adaptive responses to antimicrobial agents in biofilms. *Environ Microbiol* **2005**, *7*, 1186−1191.

(6) Driffield, K.; Miller, K.; Bostock, J. M.; O'Neill, A. J.; Chopra, I. Increased mutability of *Pseudomonas aeruginosa* in biofilms. *J. Antimicrob. Chemother.* **2008**, *61*, 1053−1056.

(7) Khan, F.; Pham, D. T. N.; Tabassum, N.; Oloketuyi, S. F.; Kim, Y. M. Treatment strategies targeting persister cell formation in bacterial pathogens. *Crit Rev Microbiol* **2020**, *46*, 665−688.

(8) Qin, S.; Xiao, W.; Zhou, C.; Pu, Q.; Deng, X.; Lan, L.; Liang, H.; Song, X.; Wu, M. *Pseudomonas aeruginosa*: pathogenesis, virulence factors, antibiotic resistance, interaction with host, technology advances and emerging therapeutics. *Signal Transduction and Targeted Therapy* **2022**, *7*, 199.

(9) Cheung, G. Y. C.; Bae, J. S.; Otto, M. Pathogenicity and virulence of *Staphylococcus aureus*. *Virulence* **2021**, *12*, 547−569.

(10) Lin, Q.; Deslouches, B.; Montelaro, R. C.; Di, Y. P. Prevention of ESKAPE pathogen biofilm formation by antimicrobial peptides WLBU2 and LL37. *Int. J. Antimicrob. Agents* **2018**, *52*, 667−672.

(11) Arciola, C. R.; Campoccia, D.; Montanaro, L. Implant infections: adhesion, biofilm formation and immune evasion. *Nat. Rev. Microbiol.* **2018**, *16*, 397−409.

(12) Vestby, L. K.; Grønseth, T.; Simm, R.; Nesse, L. L. Bacterial Biofilm and its Role in the Pathogenesis of Disease. *Antibiotics* **2020**, *9*, 59.

(13) Ozdal, M.; Gurkok, S. Recent advances in nanoparticles as antibacterial agent. *Admet dmpk* **2022**, *10*, 115−129.

(14) Mudshinge, S. R.; Deore, A. B.; Patil, S.; Bhalgat, C. M. Nanoparticles: Emerging carriers for drug delivery. *Saudi Pharm. J.* **2011**, *19*, 129−141.

(15) Khorsandi, K.; Hosseinzadeh, R.; Sadat Esfahani, H.; Keyvani-Ghamsari, S.; Ur Rahman, S. Nanomaterials as drug delivery systems with antibacterial properties: current trends and future priorities. *Expert Rev. Anti-Infect. Ther.* **2021**, *19*, 1299−1323.

(16) Pandit, C.; Roy, A.; Ghotekar, S.; Khusro, A.; Islam, M. N.; Emran, T. B.; Lam, S. E.; Khandaker, M. U.; Bradley, D. A. Biological agents for synthesis of nanoparticles and their applications. *J. King Saud Univ., Sci.* **2022**, *34*, 101869.

(17) Duan, H.; Wang, D.; Li, Y. Green chemistry for nanoparticle synthesis. *Chem. Soc. Rev.* **2015**, *44*, 5778−5792.

(18) Khan, F.; Jeong, G.-J.; Singh, P.; Tabassum, N.; Mijakovic, I.; Kim, Y.-M. Retrospective analysis of the key molecules involved in the green synthesis of nanoparticles. *Nanoscale* **2022**, *14*, 14824−14857.

(19) Jeong, G. J.; Khan, S.; Tabassum, N.; Khan, F.; Kim, Y. M. Marine-Bioinspired Nanoparticles as Potential Drugs for Multiple Biological Roles. *Mar. Drugs* **2022**, *20*, 527.

(20) Barcenilla, C.; Ducic, M.; López, M.; Prieto, M.; Álvarez-Ordóñez, A. Application of lactic acid bacteria for the biopreservation of meat products: A systematic review. *Meat Sci.* **2022**, *183*, 108661.

(21) Mokoena, M. P.; Omatola, C. A.; Olaniran, A. O. Applications of Lactic Acid Bacteria and Their Bacteriocins against Food Spoilage Microorganisms and Foodborne Pathogens. *Molecules* **2021**, *26*, 7055.

(22) Daba, G. M.; Elkhateeb, W. A. Bacteriocins of lactic acid bacteria as biotechnological tools in food and pharmaceuticals: Current applications and future prospects. *Biocatal. Agric. Biotechnol.* **2020**, *28*, 101750.

(23) Maragkoudakis, P. A.; Chingwaru, W.; Gradisnik, L.; Tsakalidou, E.; Cencic, A. Lactic acid bacteria efficiently protect human and animal intestinal epithelial and immune cells from enteric virus infection. *Int. J. Food Microbiol.* **2010**, *141*, S91−S97.

(24) Vieco-Saiz, N.; Belguesmia, Y.; Raspoet, R.; Auclair, E.; Gancel, F.; Kempf, I.; Drider, D. Benefits and Inputs From Lactic Acid Bacteria and Their Bacteriocins as Alternatives to Antibiotic Growth Promoters During Food-Animal Production. *Front. Microbiol.* **2019**, *10*, 57.

(25) Mohammed, A. B. A.; Hegazy, A. E.; Salah, A. Novelty of synergistic and cytotoxicity activities of silver nanoparticles produced by *Lactobacillus acidophilus*. *Appl. Nanosci.* **2023**, *13*, 633−640.

(26) Kang, M.-G.; Khan, F.; Jo, D.-M.; Oh, D.; Tabassum, N.; Kim, Y.-M. Antibiofilm and Antivirulence Activities of Gold and Zinc Oxide Nanoparticles Synthesized from Kimchi-Isolated *Leuconostoc* sp. Strain C2. *Antibiotics* **2022**, *11*, 1524.

(27) Nas, F.; Aissaoui, N.; Mahjoubi, M.; Mosbah, A.; Arab, M.; Abdelwahed, S.; Khrouf, R.; Masmoudi, A. S.; Cherif, A.; Klouche-Khelil, N. A comparative GC-MS analysis of bioactive secondary metabolites produced by halotolerant *Bacillus* spp. isolated from the Great Sebkha of Oran. *Int. Microbiol.* **2021**, *24*, 455−470.

(28) Rice, L. B. Federal funding for the study of antimicrobial resistance in nosocomial pathogens: no ESKAPE. *J. Infect. Dis.* **2008**, *197*, 1079−1081.

(29) Liu, Y.; Kim, S.; Kim, Y. J.; Perumalsamy, H.; Lee, S.; Hwang, E.; Yi, T. H. Green synthesis of gold nanoparticles using Euphrasia officinalis leaf extract to inhibit lipopolysaccharide-induced inflammation through NF-κB and JAK/STAT pathways in RAW 264.7 macrophages. *Int. J. Nanomed.* **2019**, *14*, 2945−2959.

(30) Nagalingam, M.; Kalpana, K.; Devi Rajeswari, V.; Panneerselvam, A. Biosynthesis, characterization, and evaluation of bioactivities of leaf extract-mediated biocompatible gold nanoparticles from *Alternanthera bettzickiana*. *Biotechnol. Rep.* **2018**, *19*, No. e00268.

(31) Chouhan, S.; Guleria, S. Green synthesis of AgNPs using *Cannabis sativa* leaf extract: Characterization, antibacterial, anti-yeast and α-amylase inhibitory activity. *Mater. Sci. Energy Technol.* **2020**, *3*, 536−544.

(32) Van Giau, V.; An, S. S. A.; Hulme, J. Recent advances in the treatment of pathogenic infections using antibiotics and nano-drug delivery vehicles. *Drug Des., Dev. Ther.* **2019**, *13*, 327−343.

(33) Łojewska, E.; Sakowicz, T. An Alternative to Antibiotics: Selected Methods to Combat Zoonotic Foodborne Bacterial Infections. *Curr. Microbiol.* **2021**, *78*, 4037−4049.

(34) Mah, T.-F. C.; O'Toole, G. A. Mechanisms of biofilm resistance to antimicrobial agents. *Trends Microbiol.* **2001**, *9*, 34−39.

(35) Aththanayaka, S.; Thiripuranathar, G.; Ekanayake, S. Emerging advances in biomimetic synthesis of nanocomposites and potential applications. *Mater. Today Sustainability* **2022**, *20*, 100206.

(36) Thiruvengadam, M.; Rajakumar, G.; Chung, I. M. Nanotechnology: current uses and future applications in the food industry. *3 Biotech* **2018**, *8*, 74.

(37) Ahmed, S. F.; Mofijur, M.; Rafa, N.; Chowdhury, A. T.; Chowdhury, S.; Nahrin, M.; Islam, A. B. M. S.; Ong, H. C. Green approaches in synthesising nanomaterials for environmental nanobioremediation: Technological advancements, applications, benefits and challenges. *Environ. Res.* **2022**, *204*, 111967.

(38) Kechagia, M.; Basoulis, D.; Konstantopoulou, S.; Dimitriadi, D.; Gyftopoulou, K.; Skarmoutsou, N.; Fakiri, E. M. Health benefits of probiotics: a review. *ISRN Nutr.* **2013**, *2013*, 481651.

https://doi.org/10.1021/acsomega.2c06789
ACS Omega 2023, 8, 9873−9888

(39) Yang, E. J.; Chang, H. C. Purification of a new antifungal compound produced by *Lactobacillus plantarum* AF1 isolated from kimchi. *Int. J. Food Microbiol.* **2010**, *139*, 56−63.
(40) Čechovská, L.; Cejpek, K.; Konečný, M.; Velíšek, J. On the role of 2,3-dihydro-3,5-dihydroxy-6-methyl-(4H)-pyran-4-one in antioxidant capacity of prunes. *Eur. Food Res. Technol.* **2011**, *233*, 367−376.
(41) Yu, X.; Zhao, M.; Liu, F.; Zeng, S.; Hu, J. Identification of 2,3-dihydro-3,5-dihydroxy-6-methyl-4H-pyran-4-one as a strong antioxidant in glucose-histidine Maillard reaction products. *Food Res. Int.* **2013**, *51*, 397−403.
(42) Chaudhari, P. R.; Masurkar, S. A.; Shidore, V. B.; Kamble, S. P. Antimicrobial Activity of Extracellularly Synthesized Silver Nanoparticles using *Lactobacillus* species Obtained from VIZYLAC Capsule. *J. Appl. Pharmaceut. Sci.* **2012**, *2*, 25−29.
(43) Rajesh, S.; Dharanishanthi, V.; Kanna, A. V. Antibacterial mechanism of biogenic silver nanoparticles of *Lactobacillus acidophilus*. *J. Exp. Nanosci.* **2015**, *10*, 1143−1152.
(44) Dakhil, A. S. Biosynthesis of silver nanoparticle (AgNPs) using *Lactobacillus* and their effects on oxidative stress biomarkers in rats. *J. King Saud Univ., Sci.* **2017**, *29*, 462−467.
(45) Viorica, R.-P.; Pawel, P.; Kinga, M.; Michal, Z.; Katarzyna, R.; Boguslaw, B. *Lactococcus lactis* as a safe and inexpensive source of bioactive silver composites. *Appl. Microbiol. Biotechnol.* **2017**, *101*, 7141−7153.
(46) Khan, F.; Kang, M. G.; Jo, D. M.; Chandika, P.; Jung, W. K.; Kang, H. W.; Kim, Y. M. Phloroglucinol-Gold and -Zinc Oxide Nanoparticles: Antibiofilm and Antivirulence Activities towards *Pseudomonas aeruginosa* PAO1. *Mar. Drugs* **2021**, *19*, 601.
(47) Sharma, S.; Sharma, N.; Kaushal, N. Comparative Account of Biogenic Synthesis of Silver Nanoparticles Using Probiotics and Their Antimicrobial Activity Against Challenging Pathogens. *Bionanosci.* **2022**, *12*, 833−840.
(48) Garmasheva, I.; Kovalenko, N.; Voychuk, S.; Ostapchuk, A.; Livins'ka, O.; Oleschenko, L. *Lactobacillus* species mediated synthesis of silver nanoparticles and their antibacterial activity against opportunistic pathogens in vitro. *Bioimpacts* **2016**, *6*, 219−223.
(49) He, S.; Zhang, Y.; Guo, Z.; Gu, N. Biological Synthesis of Gold Nanowires Using Extract of *Rhodopseudomonas capsulata*. *Biotechnol. Prog.* **2008**, *24*, 476−480.
(50) Składanowski, M.; Wypij, M.; Laskowski, D.; Golińska, P.; Dahm, H.; Rai, M. Silver and gold nanoparticles synthesized from *Streptomyces* sp. isolated from acid forest soil with special reference to its antibacterial activity against pathogens. *J. Cluster Sci.* **2017**, *28*, 59−79.
(51) He, S.; Guo, Z.; Zhang, Y.; Zhang, S.; Wang, J.; Gu, N. Biosynthesis of gold nanoparticles using the bacteria Rhodopseudomonas capsulata. *Mater. Lett.* **2007**, *61*, 3984−3987.
(52) Singh, P.; Mijakovic, I. Rowan Berries: A Potential Source for Green Synthesis of Extremely Monodisperse Gold and Silver Nanoparticles and Their Antimicrobial Property. *Pharmaceutics* **2021**, *14*, 82.
(53) Mohanta, Y. K.; Biswas, K.; Jena, S. K.; Hashem, A.; Abd_Allah, E. F.; Mohanta, T. K. Anti-biofilm and Antibacterial Activities of Silver Nanoparticles Synthesized by the Reducing Activity of Phytoconstituents Present in the Indian Medicinal Plants. *Front. Microbiol.* **2020**, *11*, 1143.
(54) Goswami, S. R.; Sahareen, T.; Singh, M.; Kumar, S. Role of biogenic silver nanoparticles in disruption of cell-cell adhesion in *Staphylococcus aureus* and *Escherichia coli* biofilm. *J. Ind. Eng. Chem.* **2015**, *26*, 73−80.
(55) Chua, S. L.; Liu, Y.; Yam, J. K.; Chen, Y.; Vejborg, R. M.; Tan, B. G.; Kjelleberg, S.; Tolker-Nielsen, T.; Givskov, M.; Yang, L. Dispersed cells represent a distinct stage in the transition from bacterial biofilm to planktonic lifestyles. *Nat. Commun.* **2014**, *5*, 4462.
(56) Flemming, H.-C.; Wingender, J. The biofilm matrix. *Nat. Rev. Microbiol.* **2010**, *8*, 623−633.
(57) Husain, F. M.; Qais, F. A.; Ahmad, I.; Hakeem, M. J.; Baig, M. H.; Masood Khan, J.; Al-Shabib, N. A. Biosynthesized Zinc Oxide Nanoparticles Disrupt Established Biofilms of Pathogenic Bacteria. *Appl. Sci.* **2022**, *12*, 710.
(58) Hentzer, M.; Wu, H.; Andersen, J. B.; Riedel, K.; Rasmussen, T. B.; Bagge, N.; Kumar, N.; Schembri, M. A.; Song, Z.; Kristoffersen, P.; Manefield, M.; Costerton, J. W.; Molin, S.; Eberl, L.; Steinberg, P.; Kjelleberg, S.; Høiby, N.; Givskov, M. Attenuation of *Pseudomonas aeruginosa* virulence by quorum sensing inhibitors. *EMBO J.* **2003**, *22*, 3803−3815.
(59) Lee, J.-H.; Cho, H. S.; Kim, Y.; Kim, J.-A.; Banskota, S.; Cho, M. H.; Lee, J. Indole and 7-benzyloxyindole attenuate the virulence of *Staphylococcus aureus*. *Appl. Microbiol. Biotechnol.* **2013**, *97*, 4543−4552.
(60) Salam, A. M.; Quave, C. L. Targeting Virulence in *Staphylococcus aureus* by Chemical Inhibition of the Accessory Gene Regulator System In Vivo. *mSphere* **2018**, *3*, No. e00500-17.
(61) Saeki, E. K.; Yamada, A. Y.; de Araujo, L. A.; Anversa, L.; Garcia, D. d. O.; de Souza, R. L. B.; Martins, H. M.; Kobayashi, R. K. T.; Nakazato, G. Subinhibitory Concentrations of Biogenic Silver Nanoparticles Affect Motility and Biofilm Formation in *Pseudomonas aeruginosa*. *Front. Cell. Infect. Microbiol.* **2021**, *11*, 656984.
(62) Khan, F.; Pham, D. T. N.; Oloketuyi, S. F.; Kim, Y. M. Regulation and controlling the motility properties of *Pseudomonas aeruginosa*. *Appl. Microbiol. Biotechnol.* **2020**, *104*, 33−49.
(63) Kumar, S.; Paliya, B. S.; Singh, B. N. Superior inhibition of virulence and biofilm formation of *Pseudomonas aeruginosa* PAO1 by phyto-synthesized silver nanoparticles through anti-quorum sensing activity. *Microb. Pathog.* **2022**, *170*, 105678.
(64) Won, S.-M.; Chen, S.; Park, K. W.; Yoon, J.-H. Isolation of lactic acid bacteria from kimchi and screening of Lactobacillus sakei ADM14 with anti-adipogenic effect and potential probiotic properties. *LWT* **2020**, *126*, 109296.
(65) Fazlurrahman; Batra, M.; Pandey, J.; Suri, C. R.; Jain, R. K. Isolation and characterization of an atrazine-degrading *Rhodococcussp*. strain MB-P1 from contaminated soil. *Lett. Appl. Microbiol.* **2009**, *49*, 721−729.
(66) Tamura, K.; Stecher, G.; Kumar, S. MEGA11: Molecular Evolutionary Genetics Analysis Version 11. *Mol. Biol. Evol.* **2021**, *38*, 3022−3027.
(67) Khan, F.; Oh, D.; Chandika, P.; Jo, D. M.; Bamunarachchi, N. I.; Jung, W. K.; Kim, Y. M. Inhibitory activities of phloroglucinol-chitosan nanoparticles on mono- and dual-species biofilms of *Candida albicans* and bacteria. *Colloids Surf., B* **2022**, *211*, 112307.
(68) Jo, D.-M.; Park, S.-K.; Khan, F.; Kang, M.-G.; Lee, J.-H.; Kim, Y.-M. An approach to extend the shelf life of ribbonfish fillet using lactic acid bacteria cell-free culture supernatant. *Food Control* **2021**, *123*, 107731.
(69) Khan, F.; Lee, J.-W.; Manivasagan, P.; Pham, D. T. N.; Oh, J.; Kim, Y.-M. Synthesis and characterization of chitosan oligosaccharide-capped gold nanoparticles as an effective antibiofilm drug against the *Pseudomonas aeruginosa* PAO1. *Microb. Pathog.* **2019**, *135*, 103623.
(70) Konaté, K.; Hilou, A.; Mavoungou, J. F.; Lepengué, A. N.; Souza, A.; Barro, N.; Datté, J. Y.; M'Batchi, B.; Nacoulma, O. G. Antimicrobial activity of polyphenol-rich fractions from *Sida alba* L. (Malvaceae) against co-trimoxazol-resistant bacteria strains. *Ann. Clin. Microbiol. Antimicrob.* **2012**, *11*, 5.
(71) Khan, F.; Lee, J. W.; Pham, D. T. N.; Lee, J. H.; Kim, H. W.; Kim, Y. K.; Kim, Y. M. Streptomycin mediated biofilm inhibition and suppression of virulence properties in *Pseudomonas aeruginosa* PAO1. *Appl. Microbiol. Biotechnol.* **2020**, *104*, 799−816.
(72) Essar, D. W.; Eberly, L.; Hadero, A.; Crawford, I. P. Identification and characterization of genes for a second anthranilate synthase in *Pseudomonas aeruginosa*: interchangeability of the two anthranilate synthases and evolutionary implications. *J. Bacteriol.* **1990**, *172*, 884−900.

https://doi.org/10.1021/acsomega.2c06789
ACS Omega 2023, 8, 9873−9888